Constraining a mafic thick crust model in the Andean Precordillera of the Pampean flat slab subduction region

ARTICLE *in* JOURNAL OF SOUTH AMERICAN EARTH SCIENCES · SEPTEMBER 2015

Impact Factor: 1.37 · DOI: 10.1016/j.jsames.2015.09.005

4 AUTHORS, INCLUDING:

Jean Baptiste Ammirati

National University of San Juan

6 PUBLICATIONS **4** CITATIONS

SEE PROFILE

Patricia Alvarado

National Scientific and Technical Research …

63 PUBLICATIONS **376** CITATIONS

SEE PROFILE

Journal of South American Earth Sciences xxx (2015) 1–14

Contents lists available at ScienceDirect

Journal of South American Earth Sciences

journal homepage: www.elsevier.com/locate/jsames

Constraining a mafic thick crust model in the Andean Precordillera of the Pampean flat slab subduction region

Sofía Beatriz Pérez Luján [a, *], Jean-Baptiste Ammirati [a, b], Patricia Alvarado [a], Graciela Irene Vujovich [c]

[a] Centro de Investigaciones de la Geósfera y Biósfera (CIGEOBIO), Consejo Nacional de Investigaciones Científicas y Técnicas (CONICET), Dpto. de Geofísica y Astronomía, Facultad de Ciencias Exactas, Físicas y Naturales, Universidad Nacional de San Juan, San Juan, Meglioli 1160 Sur, 5406 Rivadavia, San Juan, Argentina

[b] Agencia Nacional de Promoción Científica y Tecnológica (FONCyT), Argentina

[c] Instituto de Estudios Andinos Don Pablo Groeber (UBA-CONICET), Departamento de Ciencias Geológicas, Facultad de Ciencias Exactas y Naturales, Universidad de Buenos Aires, Buenos Aires, Argentina

ARTICLE INFO

Article history:
Received 4 January 2015
Received in revised form
31 August 2015
Accepted 4 September 2015
Available online xxx

Keywords:
Seismic velocities
Western Andean Precordillera
Continental crust
Flat slab subduction
Mafic-ultramafic lithology

ABSTRACT

Elastic properties in twelve representative rock samples from Central and Western Precordillera in the Andean backarc region of Argentina between 30 and 31°S were estimated from detailed petrological analysis. Thus, P and S seismic-wave velocities (Vp, Vs) as well as Poisson's ratio (σ) among other parameters were derived for gabbros, leuco-gabbros and wehrlites, in greenschist and amphibolite metamorphic conditions using a framework of a wide variety of empirical observations from active continental margins. In addition, Vs lithosphere models along two west–east cross sections were obtained using a joint inversion of teleseismic Rayleigh waves and receiver functions. These models clearly delineate the upper-plate crustal structure and the flat-slab subduction of the Nazca plate at about 100 km depth in this region. The suggested seismic velocity structure shows a relatively low (<3.3 km/s) Vs layer located in the first 15–18 km depth, then an increase of it from 3.3 to 4 km/s between 20 and 55 km depth with a mayor change at 40 km depth beneath the Precordillera showing an increase in Vs from 3.3 to 3.8 km/s. The Moho discontinuity was identified at around 65 km depth beneath the Precordillera (Vs = 4.3 km/s) and shows a low shear-wave velocity contrast in comparison with the upper continental mantle's parameters. Using this seismological model, Vs estimations derived from the petrological analyses for the 12 collected samples can be projected at depths greater than 30 km. These geophysical and petrological results agree with the hypothesis of a mafic thickened and partially eclogitized lower crust beneath the Precordillera, which has been predicted previously on a base of seismological studies only. Our petrological and seismological results collectively support a thick crustal model of a mafic–ultramafic composition extending to middle-to-lower crustal levels beneath Central and Western Precordillera; this region correlates with a suture zone between the eastern Cuyania terrane and the western Chilenia terrane.

1. Introduction

1.1. Geotectonic framework

The basement of the Andean backarc region between 28 and 33°S is composed of different terranes accreted to the southwestern margin of Gondwana during Paleozoic times (Ramos et al., 1986) (Fig. 1). The boundaries between them are represented by regional lineaments, mafic–ultramafic ophiolite belts, presence of ancient magmatic arcs and other tectonic features. Particularly, the composite Cuyania terrane juxtaposes the Argentinean Precordillera and the westernmost part of the Sierras Pampeanas (Vujovich et al., 2004).

The Precordillera of Argentina comprises the outer zone of the Andes between 29 and 33°S in an elongated 400 km long, 80 km

* Corresponding author. Departamento de Geofísica y Astronomía, Facultad de Ciencias Exactas, Físicas y Naturales, Universidad Nacional de San Juan, Meglioli 1160 Sur, Rivadavia 5406, San Juan, Argentina.
E-mail address: sofiap.lujan@unsj-cuim.edu.ar (S.B. Pérez Luján).

http://dx.doi.org/10.1016/j.jsames.2015.09.005
0895-9811/

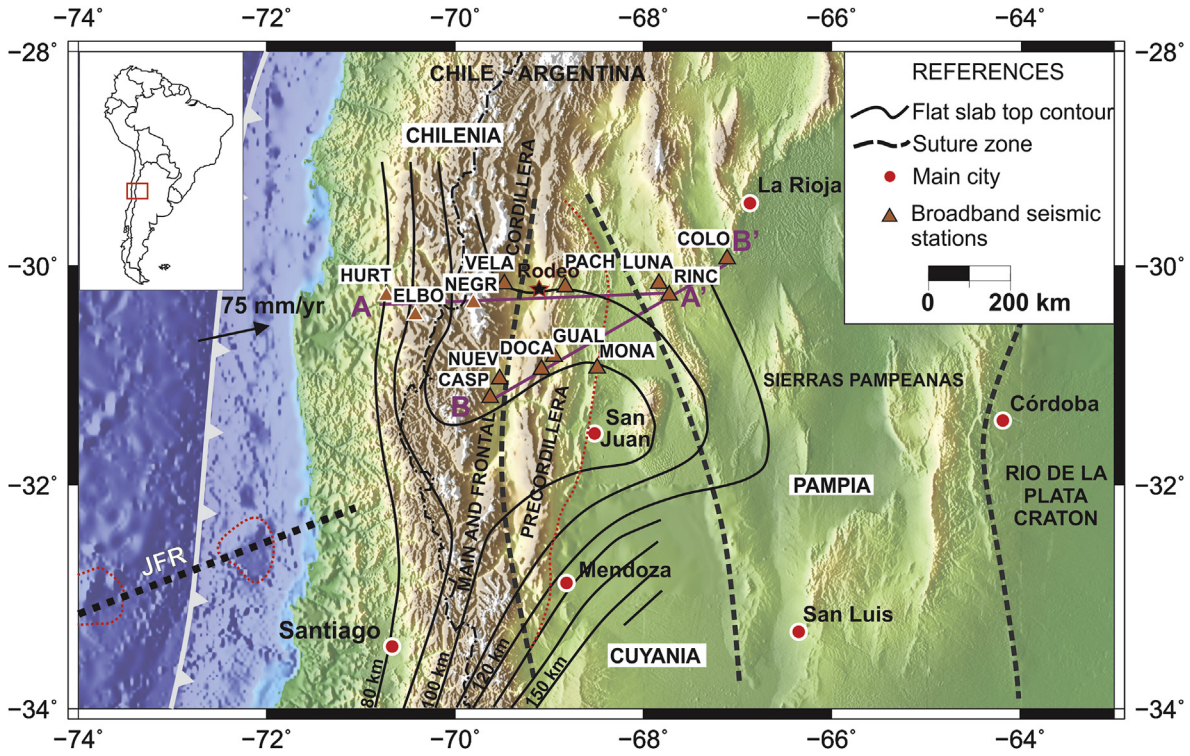

Fig. 1. Location map of the Pampean flat slab subduction region. Continuous black lines represent the top of the subducted Nazca plate (Anderson et al., 2007). Dashed black lines represent suture zones between different Paleozoic accreted terranes (see references in the text). Dotted black line represents the path of the Juan Fernández ridge (JFR). Triangles symbolize location of seismological broadband stations from CHARGE and SIEMBRA experiments (Beck et al., 2001). Convergence rate between the Nazca plate and Southamerican plate (DeMets et al., 2010) and selected cross-sections in this study (AA′ and BB′) across the morphostructural units of Main and Frontal Cordillera, Precordillera and Western Sierras Pampeanas, are also shown.

wide belt of mostly Paleozoic rocks that reaches maximum elevations of 4000 m (Ramos, 1988) (Fig. 2). It overlies an horizontal portion of the subducted Nazca plate (Cahill and Isacks, 1992; Anderson et al., 2007) and has a lack of major magmatism since 10 My (Kay et al., 1988).

This geological province can be separated into three morphostructural units based on stratigraphic and structural characteristics and their intervening valleys (Baldis and Chebli, 1969; Ortiz and Zambrano, 1981; Baldis et al., 1982). The Western and Central Precordillera constitutes an east-vergent thin-skinned belt whereas the Eastern Precordillera corresponds to a west-vergent basement block. The basement of the Central Precordillera is indirectly known from xenoliths of Miocene volcanic rocks (Leveratto, 1968), which have yielded U/Pb zircon ages near 1100 My (Kay et al., 1996; Rapela et al., 2010). In addition, the Western Sierras Pampeanas (McDonough et al., 1993) seem to be part of the same basement structure with an intra-Grenville suture (Vujovich and Kay, 1998; Vujovich et al., 2004).

The main stratigraphic difference between the three morphostructural Precordilleran units is a well-developed thick carbonate Cambrian to middle Ordovician platform sequence in the Eastern Precordillera, which changes to slope and deep sea siliciclastic facies towards the Central and Western Precordillera. These association facies are temporally and spatially related with mafic and ultramafic bodies grouped into the Precordillera mafic–ultramafic belt (Haller and Ramos, 1984; Ramos et al., 1984, 1986). This belt is represented by a series of discontinuous exposures that outcrop from north to south at La Rioja (Jagüé area), San Juan (Rodeo, Sierra del Tigre, Sierra de La Invernada and Calingasta area) and Mendoza (Peñasco, Cerro Redondo, Cortaderas, Bonilla and Guarguaraz localities) (Fig. 2).

There is a general consensus that the Western and Central Precordillera mafic–ultramafic belt and related metasedimentary rocks belong to an almost complete ophiolite sequence which has been exposed by the collision of the Chilenia terrane against the western Gondwana margin in the middle-late Devonian (Haller and Ramos, 1984; Ramos et al., 1984, 1986).

The probable continuation of the mafic–ultramafic belt to deeper levels into the crust has not been explored. This can be estimated using P and S-wave velocity determinations which are expected to be distinctive for different rock type composition, discontinuities and lithosphere structure imaging (e.g., Birch, 1960; Christensen, 1965, 1978; Poster, 1973; Peterson et al., 1974; Kroenke et al., 1976; Christensen and Mooney, 1995). Our study constrain seismic velocities as derived from detailed petrological observations and compared to seismological observations in Rodeo, Sierra del Tigre and Sierra de La Invernada area. This allows us to elaborate a structure model for the crust and deeper levels. Preliminary results studying 4 samples and a Receiver Function (RF) local model beneath one single seismic station DOCA located in the Sierra de La Invernada western flank (Ammirati et al., 2013 and Pérez Luján et al., 2013) showed a composition compatible with greenschist to amphibolite mafic rocks down to 36 km depth at medium-to-lower crustal levels, with P-wave velocities between 6.5 and 7 km/s. In this work we present a regional study considering a larger sample dataset from the Western and Central Precordillera between 30 and 31°S using a more refined seismological model involving a joint inversion of Rayleigh waves and RF along some transects. The methodology can be followed in Ammirati et al. (2015); it basically constrains absolute seismic wave velocities

Please cite this article in press as: Pérez Luján, S.B., et al., Constraining a mafic thick crust model in the Andean Precordillera of the Pampean flat slab subduction region, Journal of South American Earth Sciences (2015), http://dx.doi.org/10.1016/j.jsames.2015.09.005

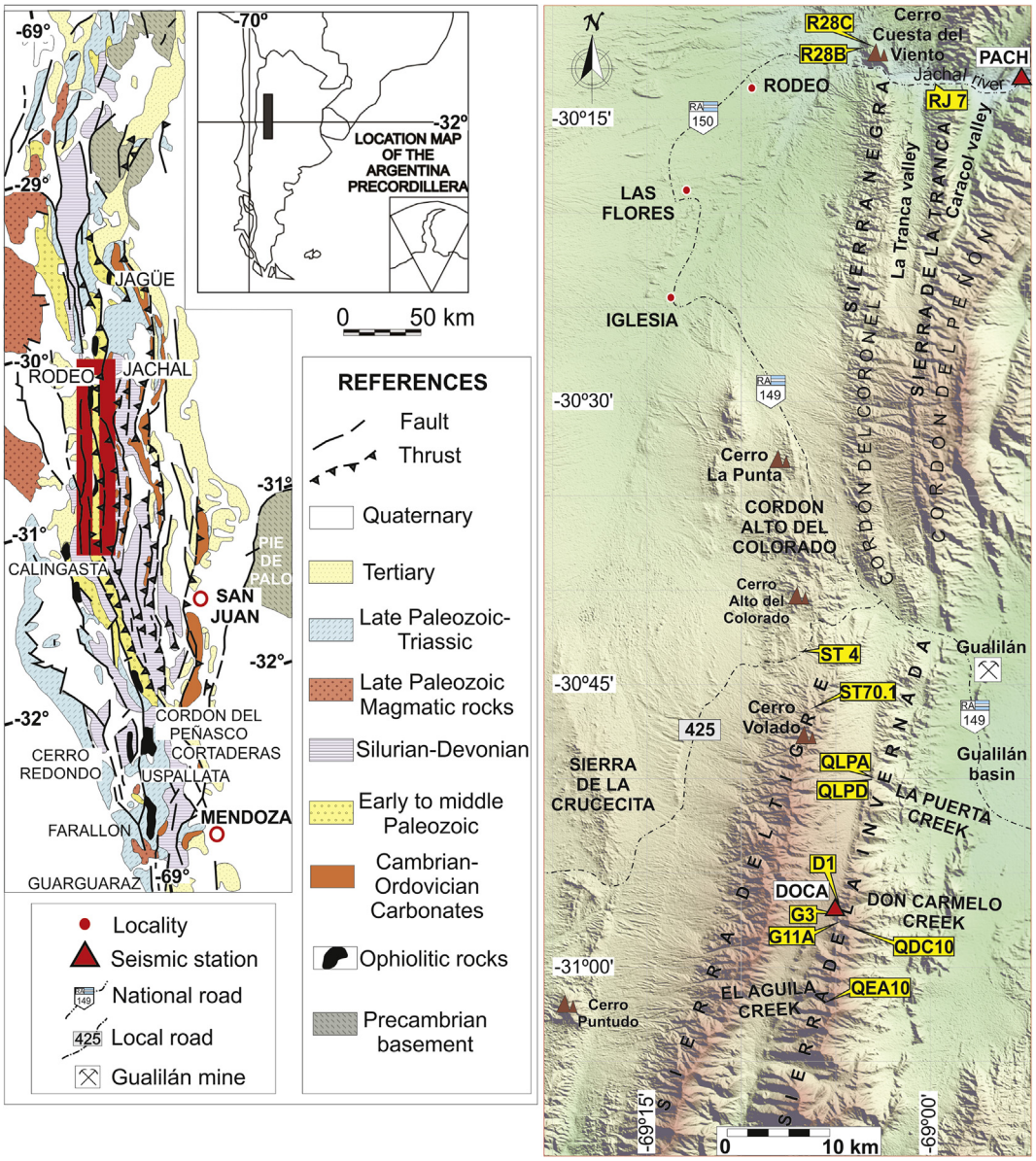

Fig. 2. Geological map of the Andean Precordillera (modified from Baldis et al., 1982) and location of the studied area (rectangle). Selected petrological samples named as in Table 1 are shown in (yellow) squares. CHARGE-SIEMBRA seismic stations installed in the Precordillera are represented by (red) triangles. (For interpretation of the references to colour in this figure legend, the reader is referred to the web version of this article.)

since RF is only sensitive to relative velocity contrasts. Thus we explore a continuation at depth of exposed lithologies in a framework of lateral velocity structure at a lithospheric scale in the Andean backarc region.

Superimposed rifting events in Late Paleozoic and Mesozoic caused extensive magmatism and extensional faulting, frequently developing sedimentary backarc basins on the hanging walls of Paleozoic terrane sutures (Franzese and Spalletti, 2001; Franzese et al., 2003). The Andean compression (2.6 Ma to present) inverted these previous extensional structures in association with the uplift of the thick-skinned Sierras Pampeanas basement-cored blocks and caused reactivation of inherited weakness fault zones (Ramos, 1994; Ramos et al., 2002). Significant deformation focused along suture zones between previously accreted terranes (Figs. 1 and 2). However, little is known about a continuation at depth of these geological observations which is the main goal of this study.

1.2. Western-Central Precordillera geological framework

The Lower Paleozoic stratigraphy in Sierra Negra (near the Rodeo locality, see Fig. 2 for location) is characterized by a large thickness of siliciclastic and volcanic Ordovician (Katian–Hirnantian age) rocks. The sedimentary and volcanic association is grouped in the Yerba Loca Formation (Astini, 1988), which consists of a turbidite succession of over 1000 m thick, interlayered and intruded by mafic–ultramafic sills and dikes. Although affected by a low grade metamorphism, primary sedimentary features can be recognized in several sections. The sedimentary lithology comprises fine-grained and coarse-grained turbidities with sandstones, shales and conglomerates. The mafic units in the western part of the Sierra Negra consist of dark-grey coloured basalts, basaltic pillow lavas and basalts with columnar and massive structures in fault contact with altered pelites of the Yerba Loca Formation. Spaces in the individual pillows and their vesicles are filled with chert and calcium carbonate. Coarse-grained gabbro sills have been found in

Please cite this article in press as: Pérez Luján, S.B., et al., Constraining a mafic thick crust model in the Andean Precordillera of the Pampean flat slab subduction region, Journal of South American Earth Sciences (2015), http://dx.doi.org/10.1016/j.jsames.2015.09.005

the Sierra Negra eastern flank as well as massive gabbros and ultramafic dykes in the Sierra de la Tranca (Fig. 2). Particularly, the Sierra del Tigre is characterized by fine-grained gabbros and basaltic pillow lavas (Haller and Ramos, 1984), as well as, coarse-grained gabbros, diorites and ultramafic bodies interbedded with greywacke and turbiditic sequences.

North–South trending Sierra de La Invernada extends for about 60 km along the westernmost section of the Central Precordillera. It consists of lower Paleozoic stratigraphic units that crop out in its western flank. It comprises five depositional lithofacies (conglomerates, sandstones, carbonates, shales, and calcareous breccias) that make up coarsening and thinning upward. Sedimentary units are interlayered with mafic rocks and show several wave reworking and micro-hummocky cross stratification that resemble a storm dominated by a shallow marine shelf scene (Basilici et al., 2003, 2005; Gomes et al., 2005; Moretti, 2009). This is different from the deep water fan model proposed for the Western Precordillera by Furque and Caballé (1985) and Spalletti et al. (1989). The mafic rocks were identified as dark-coloured gabbros of equigranular and inequigranular textures, enriched with plagioclase (labradorite and bytownite) and clinopyroxene (diopside and augite) with variable alteration degrees. The whole sequence (sedimentary and volcanic units) is part of the Sierra de la Invernada Formation (Furque and Caballé, 1985) of about 2000 m average thickness and has been assigned to Sandbian–Katian age (Furque, 1983; Caballé et al., 1992; Ortega et al., 2008). The Sierra de la Invernada Formation is in tectonic contact with large Ordovician carbonate blocks resedimented in a greenish Siluro-Devonian Corralito Formation sandstone matrix outcropping in the La Invernada range eastern flank (Furque and Caballé, 1988; Furque et al., 1990; Banchig, 1995).

Both lower Paleozoic metasedimentary and mafic–ultramafic rocks in Rodeo, Sierra de La Invernada and Sierra del Tigre show low grade metamorphism (Rubinstein et al., 1998; Robinson et al., 2005), with at 0.2–0.3 GPa and 200–350 °C estimated pressure and temperature (P–T) conditions in phrenite-pumpellyte to greenschist metamorphism facies. The sedimentary–igneous association resembles the upper and medium section of an ophiolite complex (Penrose definition in Anonymous, 1972, p.24), where sedimentary, basalts and gabbroic rocks are the main lithology. In addition, the southern section of the mafic–ultramafic belt located south of 33°S in Mendoza exhibits serpentinized ultramafic and mafic granulites (layered gabbros), massive gabbros, pillow lavas, basaltic dikes and sills and metahyaloclastic as a common lithology. This rock association presents metamorphic conditions stabilized in greenschist facies but others have reached higher P-T conditions of 850–1000 °C at pressures of >0.9 GPa, consistent with granulite facies (Davis et al., 1999; Boedo et al., 2012; Willner et al., 2011) and represents the medium and lower part of the same ophiolite complex.

1.3. Previous seismological observations

The complex geotectonic evolution during Paleozoic and Mesozoic in the central Andean backarc region is still difficult to understand. Many ancient structures and terrane compositions may be controlling present deformation and mountain building processes. It is worth to mention that large crustal earthquakes in the past centuries had their epicentres in the Andean Precordillera region, with a typical style of deformation showing reverse focal mechanism solutions for magnitudes above 5.0 (Alvarado et al., 2010). These studies show that some structures are capable of nucleating seismicity involving basement brittle behaviour as deep as 40 km in the Precordilleran continental crust (Ammirati et al., 2013).

Since there is an increasing interest in studying the structure and crustal composition in active margins, seismological studies have been performed in the Andean flat slab subduction region, showing the structure and inferring its mineralogical composition (e.g. Regnier et al., 1992; Smalley et al., 1993; Alvarado et al., 2005b; Gilbert et al., 2006; Calkins et al., 2006; Castro de Machuca et al., 2012; Perarnau et al., 2012; Ammirati et al., 2013). Barazangi and Isacks (1976), Cahill and Isacks (1992), Pardo et al. (2002) Anderson et al. (2007) and Marot et al. (2014) have shown the Nazca plate lies horizontally at about 100 km depth beneath the Precordillera in good agreement with the projection inland of the Juan Fernandez ridge (Yañez et al., 2001). Gilbert et al. (2006) and Gans et al. (2011) have performed a regional RF analysis to investigate the lithospheric structure along a transect at about 30°S. A more detailed RF study of teleseismic waves beneath the Western Sierras Pampeanas indicates a crustal thickness of about 47 km (Calkins et al., 2006; Perarnau et al., 2010) and 66 km beneath the Western Precordillera (Ammirati et al., 2013). This variable depth of the Moho RF signal is accompanied by a low impedance in seismic velocities and densities with respect to upper mantle properties. For this reason, those authors have suggested the presence of a partially eclogitized lower crust beneath the Cuyania terrane, consistent with isostatic models (Alvarado et al., 2009).

Ammirati et al. (2013) used RF analysis to study the crustal structure beneath DOCA seismological station (Figs. 1 and 2). They mention two mid-crustal discontinuities at 21 and 36 km depths, and the Moho discontinuity at 66 km depth, which seems to be a high value for the Precordilleran region of 4000 m average topography elevation. This study suggested the seismic discontinuities could be related to décollement levels between the Precordillera sedimentary units and the Cuyania basement. No calibration of this 1D seismic velocity structure beneath one single DOCA station (Figs. 1 and 2) has yet been attempted.

On the other hand, body wave seismic tomography studies by Wagner et al. (2005) shows high shear-wave speeds in the upper mantle above the flat slab segment, suggesting an unusual dry and cold upper mantle. However, Marot et al. (2014) put more constraints on the petrological composition of the continental mantle above the flat slab region finding evidence for slightly more probabilities of hydration. They combined seismic tomography with 2D instantaneous thermo-mechanical modelling, and predicted rock compositions based on published mineral and rock elastic properties. Marot et al.'s results show that the mantle wedge in this region is mainly dry, and up to on average 20% hydrated above 60 km depth, suggesting the low but higher probability of mantle hydration beneath the Cuyania terrane.

In this paper we integrate petrological and geophysical information in order to obtain both a petrological and seismological crustal model for the Western and Central Precordillera. Our study consisted of collecting samples from the exposed Precordillera and obtaining a more refined geophysical seismic velocity structure involving modelling of surface waves and RF waveforms using several seismic stations. The aim is to predict continuation at depth of the observed lithology.

2. Data and methods

2.1. Seismic analyses

Receiver function (RF) analysis corresponding to waves from earthquakes around the world and recorded beneath 3-component broadband seismic stations were used to investigate the lithospheric seismic structure in the Precordilleran region. At teleseismic distances, rays reach the seismic stations with an almost vertically incidence and are sensitive to the structure beneath the seismometers. When crossing a discontinuity in seismic velocities, a P to S-wave conversion occurs. P and S-waves travel at different velocities and the lag between the P and Ps (converted S-wave)

Please cite this article in press as: Pérez Luján, S.B., et al., Constraining a mafic thick crust model in the Andean Precordillera of the Pampean flat slab subduction region, Journal of South American Earth Sciences (2015), http://dx.doi.org/10.1016/j.jsames.2015.09.005

arrivals is proportional to the depth of the discontinuity responsible for the conversion. Theoretically, the vertical component contains mainly information about the seismic source whereas the horizontal components contain mainly information about the earth structure. By deconvolving the radial or tangential component from the vertical component we can get rid of both source and instrumental response (Langston, 1979). The resulting signal is a series of pulses retaining information of the structure beneath the seismometer. By inverting RFs it is possible to retrieve the wave velocity structure beneath the region of study although the result would be non-unique and strongly dependent on the initial velocity model used for the inversion; in fact, RFs are only sensitive to relative velocity contrasts between two layers. To overcome this non-uniqueness problem a joint inversion of RFs and surface wave dispersion (SW) measurements have shown overall successful results (Julià et al., 2000).

We computed teleseismic RFs for earthquakes recorded during the CHARGE (**CH**ile **AR**gentina **G**eophysical **E**xperiment) (Beck et al., 2001) and the SIEMBRA (**SI**erras **P**ampeanas **E**xperiment using **M**ulticomponent **BR**oadband **A**rray) experiments (SIEMBRA, 2015) for 13 stations in the Andean backarc. The SIEMBRA network began continuously recording in December 2007 and ran for 2 years. The previous project CHARGE was deployed for about 1.5 year between 2000 and 2002. Details about data preparation and the involved deconvolution method, which is used for computing RFs can be found in previous studies performed in this same region (e.g. Gilbert et al., 2006; Perarnau et al., 2010; Ammirati et al., 2013, 2015). As a result, a total of 275 usable RFs have been obtained. A total of 146 traces used a Gaussian filter width of 1; another group of 129 traces used a Guassian filter width of 2.5, which correspond to low-pass filters of corner frequency 0.5 and 1.2 Hz, respectively. The average number of traces per station is 21.

Rayleigh phase velocity dispersion analysis has been determined for the region of study following the methodology described in Ammirati et al. (2015). SW dispersion is sensitive to the long period variations of absolute shear-wave velocities and are thus, very useful for constraining absolute wave velocities when inverted together with RFs. In this study, dispersion curves have been determined for a 10–100 s period range.

The two datasets were then jointly inverted according to the methodology proposed by Julià et al. (2000) and Herrmann and Ammon (2002) yielding a total of 13 individual shear-wave velocity models. Each 1D obtained model corresponds to each of the 13 seismic stations shown in Fig. 1. In order to extrapolating seismic information between the stations, we used Delaunay triangulation (Watson, 1982). Thus, we built two cross-sections (AA′ and BB′ in Fig. 1) showing the lithospheric velocity structure down to 150 km depth, whose results are described in more detail below. Cross section AA′, extending along an approximate west–east trending from 30.296°S to 70.712°W and 30.272°S–67.724°W, embraces the Main and Frontal Cordillera in the west, Precordillera and the Western Sierras Pampeanas in the east. Another cross-section BB′, is oriented with and azimuth of 60° and ends at 31.210°S–69.629°W and 29.938°S–67.110°W along the path of the subducting Juan Fernandez ridge (Fig. 1).

2.2. Petrological analyses

Twelve representative rock samples were collected from mafic and ultramafic sills and dikes of the Sierra de La Invernada and Yerba Loca Formations representative from Sierra de La Invernada, Sierra del Tigre and Sierra Negra (Fig. 2). We carried out a modal mineralogical content analysis for the samples, which required sample preparation and optical methods. This involved conventional point counting of thin sections (1500 points for each thin section) using an optical polarized microscope and a James Swift model E semi-automatic point counter. Primary and secondary mineral assemblages, main textures and rock type classification were defined according to the Commission on the Systematics of Igneous Rocks (e.g., Le Maitre, 1989) (Table 1, Fig. 3). Thus, we obtained useful mineralogical information summarized in Table 1 and Fig. 3 for rock types identified on a base of modal mineralogy data.

Overall the mafic and ultramafic sampled bodies consist of north–south trending sills or lens of thickness between 50 and 150 m, interlayered with greywacke and siliciclastic units that show thin dark chilled margins of less than 5 cm. The sampled lithology (Table 1) consists of nine enriched plagioclase and clinopyroxene gabbros, one leuco-gabbro (sample QDC10), one tonalite (sample ST70.1) and one partially serpentinized wehrlite (sample RJ7). Some surface outcrop samples present massive and onion skin weathering textures according to their grain size (Fig. 4A,D,G). Sample in Fig. 4A exhibits dioritic vein systems reaching around 6 cm thickness. Thin sections are characterized by hipydiomorphic different crystal sizes with ophitic to subophitic and sometimes poikilitic domains (Fig. 4B,C,E,F,H,I). We note that the primary mineral association for all of the samples consists of clinopyroxene (augite and diopside), Ca-rich plagioclase (An_{66-75}), opaque minerals (magnetite, titanite and ilmenite), with sporadic quartz, olivine and hornblende.

Only one partially serpentinized wehrlite (sample RJ7) from the Rodeo area (Figs. 1 and 2) has been found, which contains euhedral relict crystals of olivine, clinopyroxene and serpentine (Table 1 and Fig. 3). Remaining samples belong to gabbroic rocks that show low pervasive alteration of the primary mineral assemblage. Plagioclase is variably altered to epidote, calcite, sericite and chlorite. Olivine is present as relict crystals with serpentine-group mineral alteration. Clinopyroxene is mostly fresh and sometimes presents embayed texture with a groundmass of secondary minerals (one example in thin section can be seen in Fig. 4B,C for sample D1 in Fig. 2 and Table 1).

Pressure, temperature, fluid and bulk rock compositions are directly related to metamorphic mineral assemblage. In this study we observed mineral associations for greenschist to amphibolite facies metamorphic conditions (Yardley, 1989; Bucher and Frey, 1994), consistent with pressure and temperature (P-T) peak conditions representative of medium to lower continental crustal levels.

Using bulk sample analysis results of minerals in each rock sample (Table 1) and assuming their P-T conditions, geophysical parameters were predicted as shown in Table 2 using a comparison with a full database of different rock types formed at different P-T conditions (i.e. different depths) in subduction zones (Hacker and Abers, 2004; Hacker et al., 2003). The Hacker and Abers' (2004)s rock and mineral database provides compositional details for many common subduction rock types, including 25 MORB-type rocks (Middle Ocean Rift Basalts), 19 hydrated peridotites (10 harzburgites and lherzolites) and 21 anhydrated peridotites (10 lherzolites, 7 harzburgites, 1 dunite, wherlite, olivine clinopyroxenite and pyrolite). In our petrological model, we tested for Hacker and Abers' (2004) rock compilation and samples from Western and Central Precordillera with an uncertainty range of 50 °C in temperature and 0.5 GPa in pressure according with greenschist to amphibolite facies metamorphic conditions. The physical and seismic properties (Vp, Poisson's ratio σ and density among other parameters) are predicted for each rock sample assuming its temperature and closure pressure metamorphic peak conditions at which mineral assemblages were stabilized. For the studied samples, metamorphic conditions of 0.5 GPa and 300 °C were fixed using data from the Rodeo and Calingasta areas, which exhibit similar lithology (Robinson et al., 2005). In addition, we also tested

Please cite this article in press as: Pérez Luján, S.B., et al., Constraining a mafic thick crust model in the Andean Precordillera of the Pampean flat slab subduction region, Journal of South American Earth Sciences (2015), http://dx.doi.org/10.1016/j.jsames.2015.09.005

Table 1
Modal mineralogical analyses calculated to total 100% volume, textures and rock types of representative rock samples collected from Western and Central Precordillera (Figs. 1 and 2). Samples have prefixes as follow: RJ: Río Jáchal, R: Rodeo, ST: Sierra del Tigre, QLP: Quebrada La Puerta, D: diabase, G: gabbro, QDC: Quebrada Don Carmelo, QEA: Quebrada El Águila. Abbreviations for names of rock-forming minerals are taking from Whitney and Evans (2010): Qz: quartz; Kfs: K-feldspar; Pl: plagioclase; Ol: olivine; Cpx: clinopyroxene; Hbl: hornblende; Bt: biotite; Chl: chlorite; Srp: serpentine; Ser: sericite; Cal: calcite; Opq: opaque minerals.

Sample		Location (lat./long.)	Modal composition											Primary texture	Rock type
			Primary mineralogy								Secondary mineralogy				
			Qz	kls	Pl	Ol	Cpx	Hbl	Bt	Opq	Chl	Srp	Ser	Cal	
Rodeo	RJ7	30,21752°S; 68,98918°W	0	0	0	2.73	30.8	0	0	2.53	0	63.93	0	0	Hipidiomorphic inequigranular	wehrlite
	R28B	30,18798°S; 69,05862°W	0	0	34.33	3.4	38	0	0	1.46	0	19.26	3.53	0	Hipidiomorphic equigranular	gabbro
	R28C	30,18805°S; 69,05877°W	0.81	0	46.81	0	32.25	0	0	5.12	9.12	0	5.87	0	Hipidiomorphic inequigranular subophitic	gabbro
Sierra del Tigre	ST70.1	30,76785°S; 69,10201°W	9.56	0	30.25	0	32.56	0	0	11.75	9.93	0	5.93	0	Hipidiomorphic equigranular	tonalite
	ST4	30,72263°S; 69,11028°W	3.4	0	42.33	0	39.2	0	0	3.6	0	10.53	0.93	0	Hipidiomorphic inequigranular ophitic	gabbro
Sierra de La Invernada	QLPA	30,83349°S; 69,05183°W	0	0	30.5	1.12	48.43	1.06	3.87	7.06	7.75	0	0.18	0	Hipidiomorphic inequigranular ophitic	gabbro
	QLPD	30,83363°S; 69,05153°W	0	0	52.2	2.86	29.66	0.8	0	1.33	11.6	0	1.06	0.46	Hipidiomorphic inequigranular ophitic	gabbro
	D1	30,94988°S; 69,08248°W	0.66	0	34.33	0	37.8	0	0	5	16.13	0	6.06	0	Hipidiomorphic inequigranular ophitic–subophitic	gabbro
	G3	30,95023°S; 69,08248°W	2.6	2.86	42.13	0	35.26	0	0	4.06	12.33	0	0.46	0.26	Hipidiomorphic inequigranular ophitic and poikilitic	gabbro
	QDC10	30,9563°S; 69,07148°W	3.4	0	47.13	0	24.13	0	0	5.46	13.06	0	6.66	0.13	Hipidiomorphic equigranular fine grained	leuco-gabbro
	G11A	30,96011°S; 69,08165°W	3.4	0	48	0	31.4	1.33	0	6.73	6.33	0	2.8	0	Hipidiomorphic inequigranular ophitic	gabbro
	QEA10	31,01375°S; 69,08839°W	0	0	55.6	6.53	35.73	0	0	1.66	0.46	0	0	0	Hipidiomorphic inequigranular ophitic–subophitic	gabbro

metamorphic conditions of lower continental crust levels (1.5 GPa and 500 °C) (Bucher and Grapes, 2011) (Table 2), considering these P-T conditions were estimated for the same lithology in the southern part of the mafic–ultramafic belt (Peñasco, Cortaderas areas and Guarguaraz complex). It is worth to note that analysed samples show the lowest alteration grade. Thus, we minimized effects of secondary mineral assemblage, such as chlorite, sericite and serpentine-group minerals, in deriving geophysical parameters.

3. Results

We discuss the main results from the petrological and seismic analyses from collected samples in the Western and Central Precordillera. The detailed petrologic analyses showed modal abundances in thin section samples (Table 1 and Fig. 3) consisting of mafic and ultramafic lithologies. Mafic rocks between 30 and 31°S are characterized by dark massive gabbros with ophitic to subophitic texture in thin section and represent the common outcropping lithology above described in all the studied area. Ultramafic lithologies are represented by partially serpentinized wehrlite bodies containing euhedral relict crystals of olivine, clinopyroxene and serpentinewhich crop out near the Rodeo locality (Fig. 2).

As a second step, we derived useful geophysical parameters for the samples in Figs. 2 and 3 and Table 1 by comparison with Hacker and Abers's data compilation (2004). As stated before, for this purpose we assumed two sets of P-T metamorphic peak conditions of 0.5 GPa–300 °C (Robinson et al., 2005) and 1.5 GPa–500 °C (Bucher and Grapes, 2011) simulating metamorphic conditions at middle and lower continental crust levels, respectively. Our main results are shown in Table 2 and Fig. 5A and B linking rock elastic properties (Vp, Vs, density rho, Poisson's ratio σ) and mineral compositions in a framework of geophysical parameters of different lithologies, which are typical of subduction zones (e. g. Lippard et al., 1986; Browning, 1984; Ernst, 1977).

Our results for Sample RJ7, located in the northern part of the region of study (Fig. 2) show the highest Poisson's ratio ($\sigma = 0.33$), Vp of 6.42 km/s, Vs of 3.21 km/s and density of 2.87 g/cm^3 (Tables 1 and 2). These results correlate with global rock estimations for samples containing serpentine-group minerals, and are consistent with the lowest Vp, Vs and density values, but with a very high Poisson's ratio (σ) (Tables 1 and 2; Fig. 5B). Samples R28B and ST4 located in the north and middle part of the studied region (Fig. 2) present about 20% and 10% of serpentine-group mineral content (Table 1); they both exhibit high values of σ 0.30 and σ 0.29, respectively. In contrast, sample QEA10 located in the southernmost part of the region of study (Fig. 2) is characterized by an absence of these minerals but the highest modal proportion of Ca-rich plagioclase; its composition is consistent with a high compressional-wave velocity (Vp = 7.28 km/s) and a Poisson's ratio $\sigma = 0.29$.

Please cite this article in press as: Pérez Luján, S.B., et al., Constraining a mafic thick crust model in the Andean Precordillera of the Pampean flat slab subduction region, Journal of South American Earth Sciences (2015), http://dx.doi.org/10.1016/j.jsames.2015.09.005

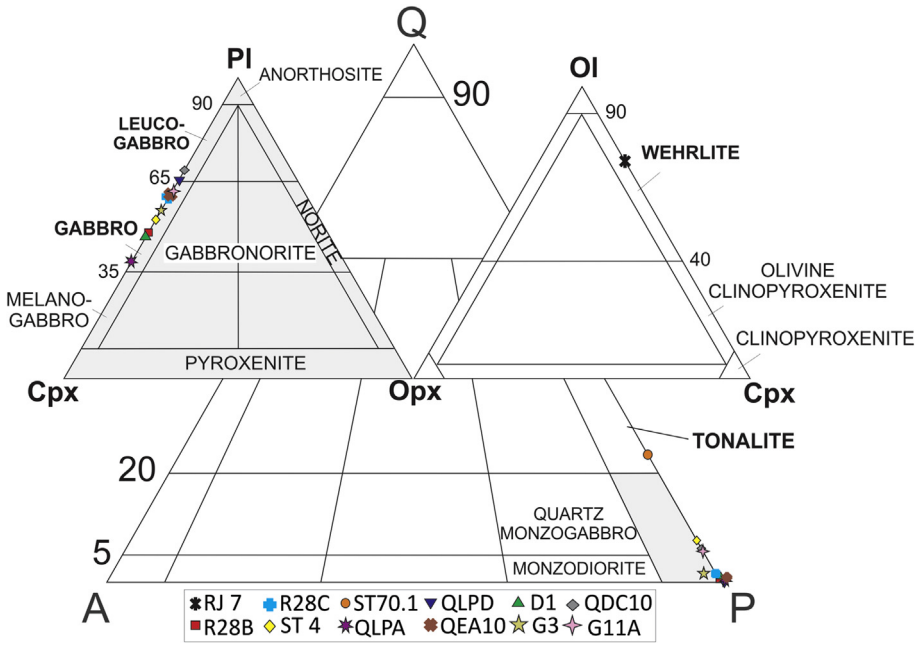

Fig. 3. Classification of rock types according to the Commission on the Systematics of Igneous Rocks (e.g. Le Maitre, 1989) projected onto the alkali feldspar (A)-quartz (Q)-plagioclase (P) plane indicating mineral content with % numbers. Superimposed are two smaller triangle diagrams of gabbroid rocks (left) based on the modal proportion of clinopyroxene (Cpx), plagioclase (P) and orthopyroxene (Opx); and of ultramafic rocks (M > 90%) (right) based on the modal proportions of olivine (Ol), orthopyroxene (Opx) and clinopyroxene (Cpx). Our samples, which are described in Table 1, mainly correspond to gabbros and leuco-gabbros. A relatively minor group of collected samples correspond to wehrlites and one tonalite.

Overall the majority of the samples in the studied area correlate with a similar composition to diabase, gabbro and olivine gabbro, which are associated with predicted geophysical parameters of approximate shear and compressional seismic wave velocities Vp between 7.07 and 7.12 km/s, Vs between 3.87 and 3.90 km/s and a Possion's ratio σ between 0.28 and 0.29. This group includes samples R28C, QLPD, D1, G3 and G11A, which show similar proportions of enriched Ca-plagioclase, clinopyroxene, sericite and chlorite, and almost absent quartz and olivine content. Also included are samples QLPA and QDC10, with estimations σ of about 0.28, Vp of 7.19 and 7.29 km/s and Vs of 3.98 and 3.99 km/s, respectively. Finally, the lowest σ value of 0.27 was calculated for sample ST70.1, located near Cerro Volado (Fig. 2) and may be the response to the presence of 10% of quartz content, which is compositionally distinguishable from other analysed rock thin sections.

Fig. 5A and B illustrate Poisson's ratio versus estimated Vp and density, respectively for medium to lower continental crust metamorphic conditions at the two sets of P-T peak conditions. Our obtained values for analysed thin section samples are comparable with olivine gabbro, diabase, gabbronorite and lithologies in greenschist and pumpellyte-actinolite metamorphic facies reported by Hacker et al. (2003) for subduction zones. Sample ST70.1 exhibits elastic properties very close to garnet amphibolites; its density and Poisson's ratio values are similar to olivine clinopyroxenite in garnet amphibolite to garnet granulite metamorphic conditions (Fig. 5B). There is a slight increase of about 1.5% in Poisson's ratio, Vp and Vs for increasing pressure and temperature.

The above mentioned results for 12 thin section samples at greenschist metamorphic conditions, have been also compared with empirical data from another compilation by Brocher (2005) of compressional and shear-wave velocities and densities related to a wide variety of common lithologies in active continental regions (Fig. 5C). This represents a dataset of elastic properties based on independent estimations of Vp, Vs and density corresponding to specific lithologies. Those estimations were obtained from laboratory and field measurements, as well as borehole, seismic vertical profiles and seismic tomography computed by different authors (e.g., Christensen, 1966, 1978; Brocher and Christensen, 2001; Brocher et al., 2004). As a result, we observed that our lithologies for the Andean Precordillera lie next to the field of metagreywackes, the mafic region (1), the metamorphic region (2) and the sedimentary rock group (5) in Fig. 5C. Remarkably, the analysed samples are in agreement with measurements for the mafic and calcium-rich rock line statistically stated by Brocher (2005). This line represents a suite of basalts, diabases, gabbros, dolomites, marbles and anorthosites with relatively higher σ values and lower shear-wave velocities (Johnson and Christensen, 1992; Christensen, 1996; Mavko et al., 1998) than estimates for average lithologies.

Fig. 5C also shows our comparison for the Central-Western Precordillera with previously obtained estimations for the continental crust of the Cuyania terrane (Alvarado et al., 2005a, 2007, 2009; Gilbert et al., 2006; Calkins et al., 2006) (Fig. 1). This terrane is located more than 100 km to the east of the Andean Precordillera here studied (Fig. 1). Except samples RJ7 and QEA10, all the studied P-wave velocities for samples range from 6.97 to 7.19 km/s and σ between 0.27 and 0.30; these values are very alike to those identified for samples in the Cuyania terrane. Taken together, these results support previous suggestions that a common basement of similar mafic composition at middle-to-lower depth crustal level lie beneath the composite (Precordilleran-Western Sierras Pampeanas) Cuyania terrane in the Andean backarc region (Castro de Machuca et al., 2012).

Geophysical observations using seismic broadband analyses allowed us to do a joint inversion of Rayleigh wave dispersion with a total of 275 usable RFs using teleseismic events of magnitudes Mw > 6 and location between 25 and 95° epicentral distances. These seismic events were recorded during the CHARGE and SIEMBRA experiments (Fig. 1). We studied two east–west cross sections with 13 individual 1D shear-wave velocity models (Fig. 1, Fig. 6A and B). The northern (AA′) and southern (BB′) transects are on top of the Andean Cordillera, Precordillera and Western Sierras Pampeanas. Two 1D models were obtained for broadband

Please cite this article in press as: Pérez Luján, S.B., et al., Constraining a mafic thick crust model in the Andean Precordillera of the Pampean flat slab subduction region, Journal of South American Earth Sciences (2015), http://dx.doi.org/10.1016/j.jsames.2015.09.005

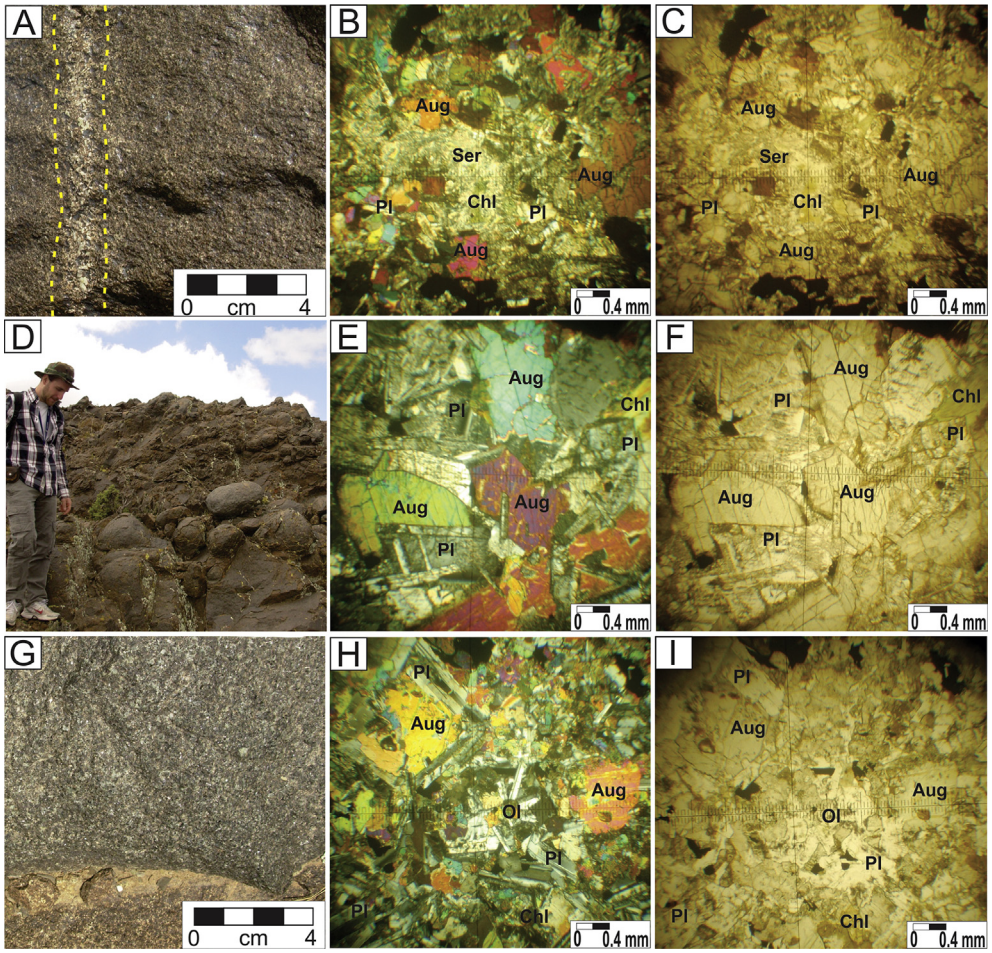

Fig. 4. A- Photograph of a thick mafic sill with north–south and east–west trending dioritic veins. B- Photomicrograph using cross-polarized light showing hipydiomorphic inequigranular ophitic texture in a partially altered gabbro. Primary (e.g., augite, plagioclase) and secondary (e.g., chlorite, sericite) mineral associations can be recognized. C- Same sample as (B) using plane-polarized light. Note the presence of secondary minerals such as chlorite (Chl) and serpentine group minerals. D- Photograph of a well-exposed coarse grained gabbro with onion skin weathering texture. E- Cross-polarized light of a thin section photomicrograph of a medium grained gabbro showing hipydiomorphic inequigranular ophitic texture and poikilitic domains. F- Same sample as (E) using plane-polarized light; note the partial alteration in primary mineral association such as plagioclase and augite with chlorite and sericite. G- Photograph of a massive gabbro. Primary mineral association can be easily recognized due to its low alteration degree and grain size. H- Photomicrograph of a thin section sample shown in (G) under cross-polarized light showing hipydiomorphic inequigranular ophitic to subophitic textures. I- Plane-polarized light thin section photomicrograph of same sample in (G). Note the presence of secondary minerals such as chlorite and serpentine replacing mafic minerals such as augite and olivine. Mineral abbreviations are from Whitney and Evans (2010): Pl: plagioclase; Ol: olivine; Aug: augite; Chl: chlorite; Ser: sericite.

Table 2
Physical property estimations (H_2O: water content in 100%; rho: density; Vp: compressional-seismic wave velocity; Vs: shear-seismic wave velocity; K: bulk modulus; G: shear modulus; Poisson's ratio σ) for samples in the Precordillera (see Fig. 2 for location and Table 1 for mineral composition) using Hashin–Shtrikman average from Hacker and Abers (2004). Two sets of P-T peak metamorphic conditions from Robinson et al. (2005) and Hacker et al. (2003) were assumed in our calculations. These predictions for high Vp, high density and high rho values are consistent with mafic – ultramafic lithologies at middle-to-lower crustal levels of the Andean Precordillera.

Geophysical parameters/samples	Rodeo			Sierra del Tigre		Sierra de la Invernada						
P = 0.5 Gpa/T = 300 °C	RJ7	R28B	R28C	ST70.1	ST4	QLPA	QLPD	D1	G3	QDC10	G11A	QEA10
H_2O (wt%)	7.86	2.53	1.19	1.27	1.34	0.95	1.24	1.90	1.27	1.62	0.80	0.05
rho (g/cm^3)	2.88	2.97	3.10	3.26	3.03	3.25	3.03	3.17	3.10	3.09	3.13	3.02
Vp (km/s)	6.42	6.97	7.07	6.99	7.02	7.19	7.12	7.08	7.07	6.94	7.07	7.29
Vs (km/s)	3.21	3.72	3.89	3.95	3.81	3.98	3.90	3.93	3.91	3.84	3.91	3.99
K (GPa)	79.16	89.43	92.41	91.47	90.48	99.48	91.87	93.55	91.67	88.25	92.84	96.23
G (GPa)	29.66	41.20	46.95	50.79	43.96	51.54	46.17	49.02	47.47	45.64	47.69	48.00
Poissons (σ)	0.33	0.30	0.28	0.27	0.29	0.28	0.28	0.28	0.28	0.28	0.28	0.29
P = 1.5 Gpa/T = 500 °C	RJ7	R28B	R28C	ST70.1	ST4	QLPA	QLPD	D1	G3	QDC10	G11A	QEA10
H_2O (wt%)	7.86	2.53	1.19	1.27	1.34	0.95	1.24	1.90	1.27	1.62	0.80	0.05
rho (g/cm^3)	2.90	2.99	3.12	3.28	3.04	3.27	3.05	3.19	3.12	3.11	3.14	3.03
Vp (km/s)	6.44	7.03	7.14	7.03	7.09	7.24	7.20	7.14	7.14	7.02	7.15	7.37
Vs (km/s)	3.20	3.75	3.92	3.95	3.85	3.99	3.95	3.95	3.95	3.87	3.94	4.04
K (GPa)	80.83	91.68	94.99	94.28	92.97	101.70	94.38	95.99	94.21	91.09	95.43	98.66
G (GPa)	29.57	41.97	48.07	51.08	45.01	52.10	47.65	49.73	48.59	46.74	48.84	49.60
Poissons (σ)	0.34	0.30	0.28	0.27	0.29	0.28	0.28	0.28	0.28	0.28	0.28	0.28

Please cite this article in press as: Pérez Luján, S.B., et al., Constraining a mafic thick crust model in the Andean Precordillera of the Pampean flat slab subduction region, Journal of South American Earth Sciences (2015), http://dx.doi.org/10.1016/j.jsames.2015.09.005

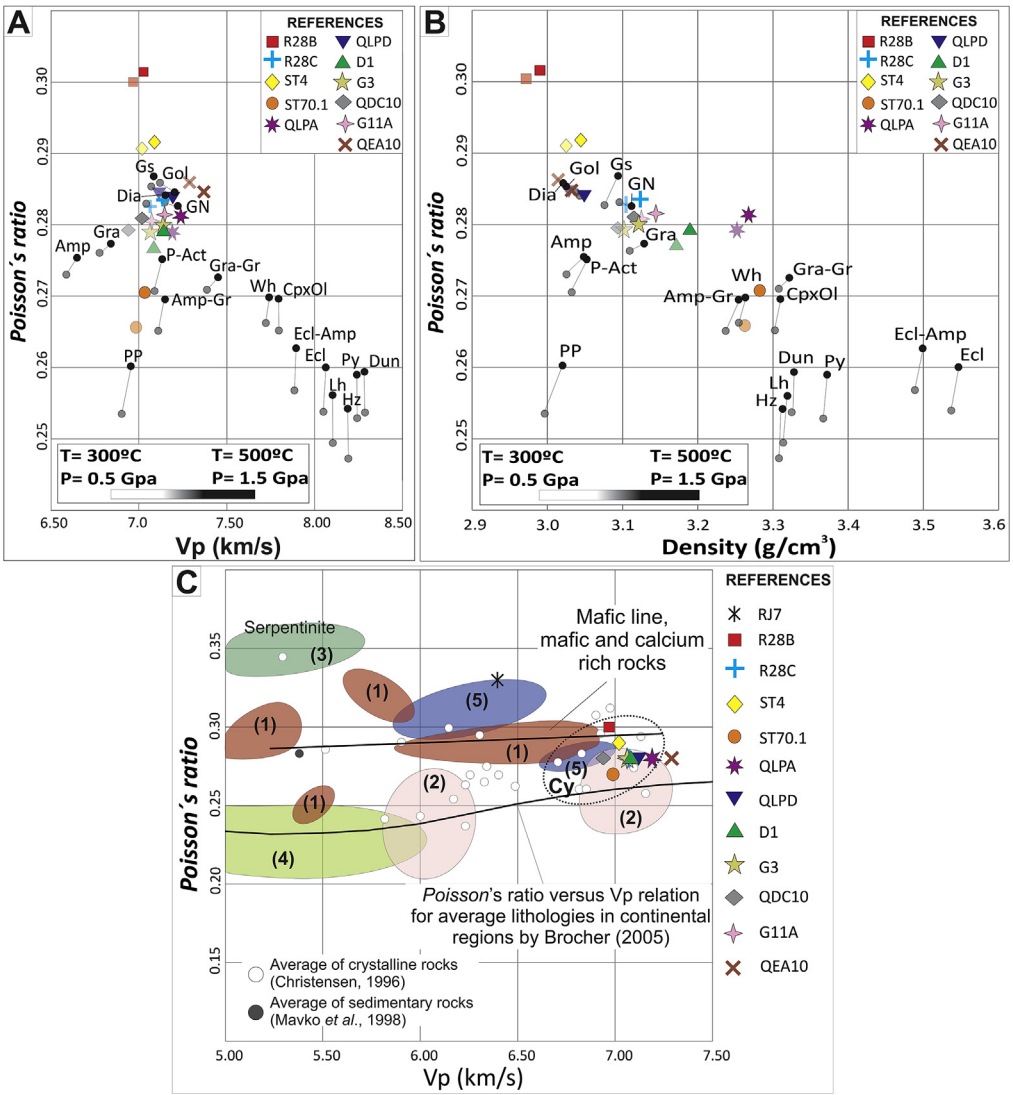

Fig. 5. A: Poisson's ratio (σ) versus compressional wave velocities (Vp) estimated for our collected samples (coloured symbols; see locations in Fig. 2 and outcrop and thin sections in Fig. 4). These geophysical parameters are derived using a comparison from Hacker and Abers (2004)'s data compilation. P-T conditions at 0.5 GPa–300 °C used for calculations are from Robinson et al. (2005). Metamorphic conditions of 1.5 GPa–500 °C are also tested considering the low alteration degree in mafic and ultramafic samples and stability field of Ca-rich plagioclase and clinopyroxene (Hacker et al., 2003) in lower crustal levels (Bucher and Grapes, 2011). Estimated values for defined mafic and ultramafic rock types typical of active continental margins (Hacker et al., 2003) are shown for reference by black circles. Rock names: Dia: diabase; GN: gabbro/norite; Gol: olivine gabbro; Wh: wehrlite; CpxOl: olivine clinopyroxenite; Py: pyrolite; Lh: lherzolite; Hz: harzburgite; Dun: dunite; PP: prehnite-pumpellyite; P-Act: pumpellyite-actinolite; Gs: greenschist; Amp-Gr: garnet amphibolite; Amp: amphibolite; Gra: granulite; Gra-Gr: garnet granulite; Ecl-Amp: amphibole eclogite; Ecl: eclogite. B: Poisson's ratio (σ) versus density (rho) results obtained for our samples (Fig. 2 and Table 1) and other lithologies reported by Hacker et al. (2003), which are representative from subduction zones assuming similar metamorphic peak conditions as in Fig. 5A. Estimated values (σ = 0.33; Vp = 6.42 km/s, rho = 2.88 g/cm^3) for Sample RJ 7 lie outside the range of the plotting area and correspond to a partial serpentinized wehrlite. Rock names as in Fig. 5A. C: Poisson's ratio (σ) as a function of Vp (P-T conditions at 0.5 GPa–300 °C used for calculations according to Robinson et al. 2005) for samples collected in Central and Western Precordillera (Figs. 2 and 3) compared with lithologies commonly found in active continental regions (Brocher, 2005). According to this author, coloured ellipses highlight measurements reported by a single reference cited in Brocher (2005); bold numbers in parentheses link ellipses: (1) metagreywackes and mafic rocks (Brocher and Chistensen, 2001); (2) metamorphic rocks (Brocher et al., 2004); (3) serpentinite rocks (Christensen and Mooney, 1995); (4) Salinian granite (Boness and Zoback, 2004); (5) sedimentary rocks (Johnson and Christensen, 1992). Ellipse in dashed line refers to estimated geophysical parameters (Vp and Poisson's ratio) for the mafic basement outcrops of the Western Sierras Pampeanas in the Cuyania (Cy) terrane (Alvarado et al., 2005a,b, 2007; 2009; Gilbert et al., 2006; Calkins et al., 2006). Note the similarity between mafic–ultramafic signal for lithologies in the Andean Precordillera when compared to estimations for the Western Sierras Pampeanas in the same Pampean flat-slab subduction region.

seismological stations located on the western flank of the Sierra de La Invernada (station DOCA in the Central Precordillera) and near Rodeo (station PACH in the Western Precordillera) (Fig. 2). In both northern (AA′) and southern (BB′) cross-sections we were able to recognize a shallower layer of a relatively low S-wave velocity (<3.3 km/s) down to 15 km depth. Cross-section AA′ shows this layer thickens from the Western Sierras Pampeanas in the east toward the west reaching 18 km depth beneath station VELA in the Main Cordillera. This same shallow layer is observed in the southern profile BB′ but in this case a maximum thickness of ~17 km is observed beneath the seismological station GUAL, which is located in Central Precordillera. This layer of low S-wave velocity could be interpreted as Paleozoic and Mesozoic sedimentary sequences, which are the main constituent of the Precordillera (Baldis and Chebli, 1969; Ortiz and Zambrano, 1981; Baldis et al., 1982). Minimum S-wave velocities observed in the northern profile are of 3.2 km/s and in the southern profile of 3.4 km/s.

A deeper S-wave layer has been recognized in both transects, located at middle to lower crustal levels. For this layer we observed an increase in shear-wave velocity (from 3.3 to 4 km/s) between

Please cite this article in press as: Pérez Luján, S.B., et al., Constraining a mafic thick crust model in the Andean Precordillera of the Pampean flat slab subduction region, Journal of South American Earth Sciences (2015), http://dx.doi.org/10.1016/j.jsames.2015.09.005

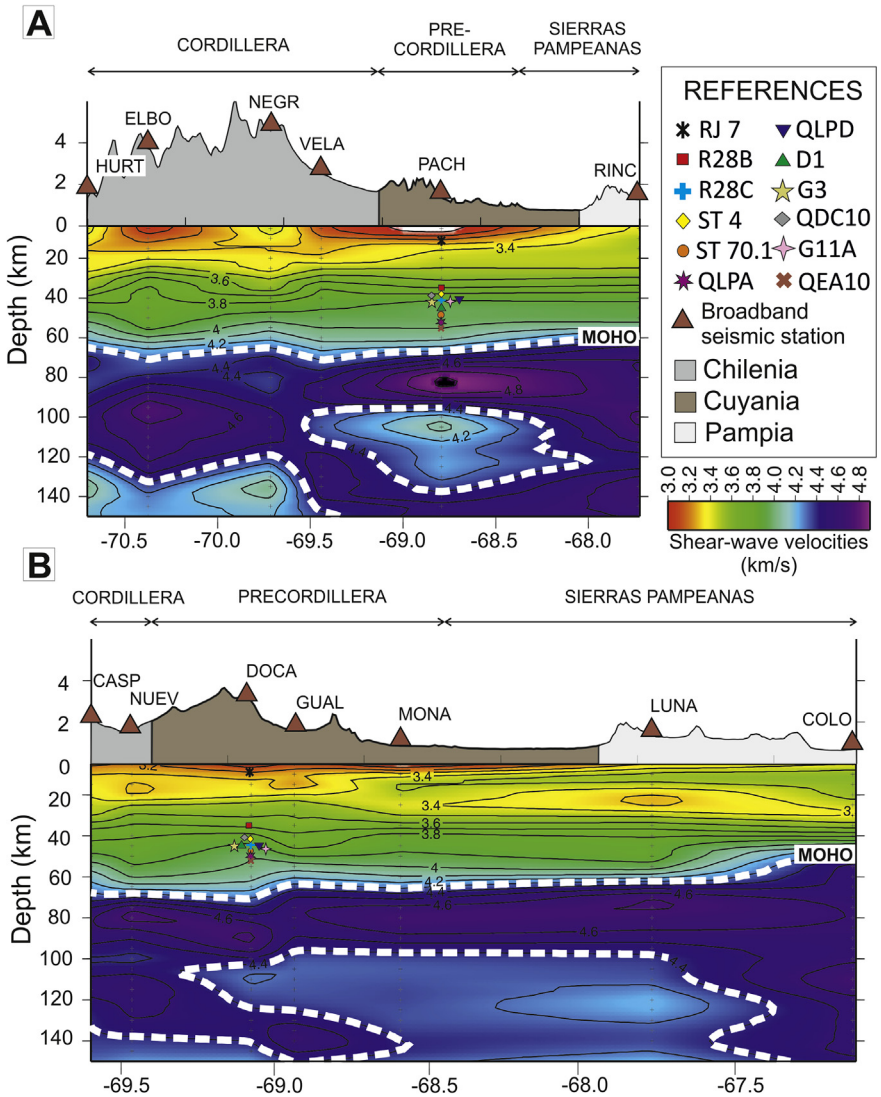

Fig. 6. Shear-wave velocity models as a function of depth obtained along two cross-sections AA′ and BB′ in the Pampean flat-slab region (see Fig. 1 for their locations). These geophysical estimations result from a joint inversion of surface waves and teleseismic receiver functions. Contours spacing is 0.1 km/s and different vertical and horizontal scales are used. In addition, coloured symbols represent our estimations in Precordillera, which indicate a mafic continental crust between 35 and 55 km depths. A- Profile AA′ is located with a west–east trending around 30°S across the Main Cordillera, Precordillera near the Rodeo locality and Western Sierras Pampeanas. B- Profile BB′ located along an azimuth of 60° across the Main Cordillera, sierra de La Invernada in Precordillera and Western Sierras Pampeanas. Note the sensitivity of geophysical determinations to Moho depths higher than 60 km beneath the Precordillera and to the subducted Nazca slab depths below 100 km depth.

~20 and 50 km depth, beneath station ELBO in Cordillera and between ~20 and 55 km depth beneath station DOCA in Central and Western Precordillera. This increase in S-wave velocity gets deeper and presents a higher contrast toward the west, probably due to changes in crustal lithology, which could involve mafic and ultramafic lithologies at higher metamorphic conditions at depth. In addition, we observed a mayor increase at about 40 km depth, with shear-wave velocity values jumping from 3.3 to 3.8 km/s in both cross-sections.

The next deeper layer in the northern and southern transects corresponds to the upper continental mantle materials with shear-wave velocities higher than 4.3 km/s. We depicted the shallower contour line of 4.3 km/s as the boundary between the lower crust and the upper continental mantle (Moho discontinuity). It is worth to note the high thickness of the continental crust beneath Cordillera, which is expected because of its high elevation reaching more than 6000 m. However, high crustal thickness are still observed more to the east beneath the Precordillera and Western Sierras Pampeanas. In northern profile the Moho changes from ~60 km depth in the Western Sierras Pampeanas (station RINC) up to ~70 km depth beneath the Main Cordillera (stations VELA and ELBO). In the southern cross-section we observe a clear Moho signal at ~47 km depth beneath Sierras Pampeanas (station COLO), which deepens at ~65 km beneath the Central and Western Precordillera (station DOCA) in a short horizontal distance of 240 km. In agreement with previous studies, the low S-wave velocity contrast at the Moho and the overthickened continental crust beneath the Cuyania basement could be explained by the believed partial eclogitization of its lower crust (Gilbert et al., 2006; Alvarado et al., 2007, 2009).

The deepest part of the seismic model exhibits low velocities between 4.1 and 4.4 km/s at depths of ~90–110 km; this is interpreted as the subducting oceanic Nazca plate. This observation is consistent with previous studies performed in the Pampean flat slab region (Gilbert et al., 2006; Gans et al., 2011; Marot et al., 2014; Ammirati et al., 2015).

We have compared our estimated shear-wave velocities in the Precordillera using the Hacker and Abers (2004) methodology with seismological observations. In the northern cross-section AA′ near

Please cite this article in press as: Pérez Luján, S.B., et al., Constraining a mafic thick crust model in the Andean Precordillera of the Pampean flat slab subduction region, Journal of South American Earth Sciences (2015), http://dx.doi.org/10.1016/j.jsames.2015.09.005

station PACH in the Western Precordillera, all collected samples (except sample RJ7) show comparable shear-wave velocities with estimations in the depth range between 30 and 50 km (Fig. 6A). In cross-sections AA′ and BB′, sample RJ7 is projected at 18 km depth according to its low shear-wave speed. But, this rock type is expected to be found at lower crustal levels where ultramafic rocks are the common lithology in average continental crust (Christensen and Mooney, 1995).

For the southern cross-section BB′, predicted S-wave velocities beneath the Precordillera for thin section analysed samples are comparable to waveform modelling Vs estimations typical of medium to lower crustal levels, which extend at depths between 35 and 50 km (Fig. 6B).

Taken together, all petrological and seismological observations provide evidence for a composition representative of a mafic–ultramafic belt, which is in good agreement with geological studies that suggest an intermediate region between the Chilenia and Cuyania terranes (Ramos et al., 1984).

4. Discussion

Several studies of bulk crustal composition in active continental margins clearly suggest the quartz enriched character associated to their most abundant granite and granodiorite rock type constituents (e.g., Christensen and Fountain, 1975; Holbrook et al., 1988, 1992; White et al., 1992; Christensen and Mooney, 1995). Some studies in the Cuyania (Sierras Pampeanas) terrane, however, have found evidence for mafic rock compositions and an overthickened crust (Gilbert et al., 2006; Calkins et al., 2006; Alvarado et al., 2009; Castro de Machuca et al., 2012; and others therein) in comparison with global average estimations (e.g., Christensen and Mooney, 1995). Our results show instead an unusual mafic crustal composition of the continental crust within the overriding continental lithosphere of the Pampean flat slab region. This mafic crust is located at about 300 km to the east of the trench in the Andean Precordillera. Thus, mafic and ultramafic lithologies such as gabbro, diabase, olivine gabbro and wehrlite seem to be the main rocks in this region at medium crustal levels. Derived geophysical parameters for 12 collected samples by comparison with Hacker and Abers's data compilation (2004) were calculated assuming two sets of P-T metamorphic peak conditions. The first peak condition stated in greenschist to amphibolite facies (0.5 GPa and 300 °C) was assumed according with the mineral paragenesis previously estimated for mafic rocks by Robinson et al. (2005) in the Rodeo and Calingasta areas. These metamorphic conditions represent medium levels of a typical continental crust and would seem most likely to occur in the upper to medium section of an ophiolite complex. Since both pressure and temperature dependencies appear to be small for mafic rocks we calculate geophysical parameters assuming a second metamorphic peak in granulite facies (1.5 GPa and 500 °C) in order to simulate P-T conditions at lower continental crust levels. For this purpose, we considered metamorphic conditions calculated by Davis et al. (1999), Willner et al. (2011) and Boedo et al. (2012) in mafic rocks from the southern part of the same ophiolite complex (Peñasco, Cortaderas and Guarguaraz areas). Even sample ST70.1 exhibits elastic properties very close to garnet amphibolites; its density and Poisson's ratio values are similar to olivine clinopyroxenite in garnet amphibolite to garnet granulite metamorphic conditions (Fig. 5B). According to Robinson et al. (2005), Davis et al. (1999) and Willner et al. (2011), the metamorphic character of the mafic–ultramafic rocks and the derived P-T conditions indicate that the metamorphism did not develop in an ocean-floor setting. Instead, the most compatible model would agree with metamorphisms developed as a result of collision between the Chilenia and Cuyania terranes in early Devonian times. If we compare our assumptions (P-T ranges of 0.5 GPa–300 °C and 1.5 GPa-500 °C) with a present day thermo-mechanical model for which the recent Andean backarc region is stable (see *Fig. 8* in Marot et al., 2014), P-T field conditions are very similar to our assumptions at medium to lower crustal levels. This indicates that the present seismic parameters calculated for a mafic–ultramafic composition are representative of the crust in this Precordilleran backarc region and would have been probably the same as those expected since Devonian.

All our results show a slight increase of about 1.5% in Poisson's ratio, Vp and Vs for increasing pressure and temperature in mafic lithologies.

On a base of S-wave velocities modelled along the two west–east transects using RF and SW joint inversion analyses, we have imaged the presence of several layers at depth, which may correlate with lithological variations. These results are different from a standard (more granitic) continental crust composition and also predict a continuation at depth of the mafic–ultramafic belt lithologies. We believe they may represent the suture zone between the Chilenia and Cuyania terrane, specifically beneath the Western and Central Precordillera.

Our shear-wave models are consistent with a relatively sharp lithological change consisting with mafic lithologies (such as leucogabbros, gabbros, olivine gabbros, wehrlites) where Ca-rich plagioclase and clinopyroxene are the major mineral constituents at mid-crustal levels.

We noted a diffuse transition between the lower crust and the upper continental mantle estimations, supporting the hypothesis of a partial eclogitization of the lower continental crust according to previous studies. It is worth to mention that seismological and petrological analysis in exposed mafic–ultramafic rocks performed by Castro de Machuca et al. (2012) in the southwestern part of the Sierra de Pie de Palo (Western Sierras Pampeanas in Figs. 1 and 2) shows similar properties as our results. Thus, calculated elastic properties for the exposed lithology in Western Sierras Pampeanas agreed with high Vp, high Vp/Vs ratio and high density in agreement with the same parameters estimated from RF analysis only for the upper and middle crust.

Our main results for all observations comprise high Vp and high Vs velocities, that could be the result of a partial eclogitized lower continental crust and an overthickened, mostly mafic–ultramafic crust in the Precordillera and Western Sierras Pampeanas region. This allows us to infer a probably common geotectonic evolution for the composite Cuyania terrane. In this region the continental crust appears to be made of oceanic accreted crust materials where quartz-enriched lithologies are comparatively poor or absent. Magnetic anomalies and gravity and isostatic modelling support these observations (Tassara et al., 2006; Chernicoff et al., 2009; Alvarado et al., 2009). Main structures and terrane compositions could have been inherited from their geotectonic history and are actually controlling the stress transfer in a highly compressive regimen (Bilbao, 2012; Monsalvo et al., 2014). In a typical continental crust the strength of the middle and lower crust can be significantly reduced due to the thermally-activated creep of wet quartz and feldspar at depths greater than the brittle–ductile transition (Rybacki et al., 2006). However, according to Zhang and Green (2007), in an overthickened mafic crust the stress transfer is mainly controlled by eclogite which dominates the rheology of the lower crust. Even, diabase and gabbros, the chemical equivalents of basalt-granulite can be as strong as olivine aggregates and eclogite when they are almost completely dry (Mackwell et al., 1998).

Crustal earthquakes in this region show moderate-to-high magnitude sizes, deep focal depths and mainly reverse or thrust faulting mechanisms (Alvarado et al., 2005a). The rheology of the

Please cite this article in press as: Pérez Luján, S.B., et al., Constraining a mafic thick crust model in the Andean Precordillera of the Pampean flat slab subduction region, Journal of South American Earth Sciences (2015), http://dx.doi.org/10.1016/j.jsames.2015.09.005

Cuyania terrane due to its mafic composition may be one the important factors controlling nucleation of crustal seismicity at deeper levels than 20 km depth (Alvarado et al., 2005b).

Another interesting observation is related to the evidence for partial lower crust eclogitization in the Cuyania terrane. The transformation of mafic rocks to eclogite involves the breakdown of plagioclase, clinopyroxene and the growth of garnet. This process could be sped up by the presence of water (Hacker, 1996). Since these are typically anhydrous minerals, it is possible to state that lower continental crust can be considered to be "dry" because these are their main constituents at deeper crustal levels (Yardley and Valley, 1997). Interestingly, studies using microscopic Fourier transform infrared spectroscopy (Micro-FTIR) have revealed that these nominally anhydrous minerals commonly contain a significant trace amount of water as OH (Yang et al., 2008; Wang et al., 2012). In this interpretation, the anomalous mafic continental crust composed of plagioclase and pyroxene may experience a breakdown process under high pressure and temperature conditions, which could release fluids (OH) accelerating metamorphic reactions and favouring the partial eclogitization of the lower continental crust. Eclogitization is inevitable if water is present and virtually impossible without it. Thus, the source of water may proceed from the mafic basement of the Cuyania terrane itself. Another important consideration in this process is that the phase transition from granulite to eclogite is accompanied by a dramatic weakening and by a loss in strength (Jackson et al., 2004). These phase transformations that involve such density changes will trigger considerable stresses that may promote failure at crustal levels. The occurrence of deep-crustal earthquakes sometimes reaching about 40 km focal depths in the mafic Cuyania terrane (Alvarado et al., 2010) could represent ongoing transformation of rocks accompanied by water release in the transition to eclogite metamorphic conditions, accelerating the generation of a weaker and denser eclogite to deeper levels in the lower crust. Thus, brittle granulite may be surrounded and mechanically isolated by weaker eclogite that can longer be fractured at this depth.

Seismicity occurrence stopping at this almost 40 km depth level can thus potentially be used as a proxy for the petro-physical processes indicating transformation to eclogite taking place at this depth representative of a brittle-fragile behaviour boundary in the continental crust of the Cuyania terrane.

5. Conclusions

Estimated elastic properties and petrological analyses of twelve representative mafic samples from Central and Western Precordillera between 30 and 31°S support the hypothesis of an anomalous continental crust beneath the Cuyania terrane and its western boundary with the Chilenia accreted terrane. Typical mafic analysed rocks correspond to gabbros, leuco-gabbros and partially serpentinized wehrlites located at middle-to-lower crustal levels in the Andean backarc of the Pampean flat-slab subduction region. We compared these lithologies with a world-wide compilation of mafic and ultramafic rocks commonly found in active continental margins, to estimate Vp, Vs, density, and Poisson's ratio parameters. The observed lithologies in Western and Central Precordillera are compatible with estimations of Vp between 6.42 and 7.37 km/s, Vs between 3.20 and 4.04 km/s, density in the 2.88 and 3.28 g/cm^3 range and Poisson's ratio between 0.27 and 0.34, assuming 0.5 GPa–300 °C and 1.5 GPa and 500 °C P-T metamorphic peak conditions. We performed two east–west cross sections of approximately 400 km length at about 30–31°S integrating 1D shear-wave velocity lithospheric models beneath 13 single broadband seismic stations. The resulting geophysical profiles using a joint inversion of P-waves teleseismic receiver functions and Rayleigh wave dispersion curves indicate different shear-wave responses in the range 3.1–4.3 km/s. This is apparently controlled by décollements levels and variations in lithology of the continental crust within the Cuyania terrane. Thus, we combined the elastic properties derived from petrological models based on sampled rocks with geophysical observations for the continental crust. Estimations at deeper levels using seismic waves but lacking a petrological analysis component allowed us to image the Mohorovich discontinuity.

Our main results for exposed and thin-section analysed sample lithologies are consistent with a pattern of deformation of a mafic–ultramafic belt for the Central and Western Precordillera region, which corresponds to the intervening (suture) zone between the Cuyania and Chilenia terranes. In addition, our analyses also predict this zone can be extended at deeper levels of about 50 km in the continental crust.

We determined a similar composition but a much thicker crust of about 66 km beneath the Western Andean Precordillera than in the Sierras Pampeanas basement located in its eastern region having crustal thickness of about 45 km; the whole area is mapping the region where the Nazca slab subducts horizontally. We suggest this can be a result of duplication of a mafic and denser crust under a compressive regimen in the Pampean flat slab region.

We observed a relatively increase in S-wave velocity in the lower crust and its low contrast with the upper continental mantle Vs' estimate. Our results support the hypothesis of partial eclogitization in the lower crust of the Cuyania terrane as previously suggested by other studies (Gilbert et al., 2006; Calkins et al., 2006) and tested by isostasy models (Alvarado et al., 2009).

A comparison between our results with estimations in the Western Sierras Pampeanas from Castro de Machuca et al. (2012), which used a similar petrological-seismic analysis, indicates the crust has a strong mafic–ultramafic character in both regions and exhibits a thickness significantly greater than average for continental regions. Although not an extensive testing, these constrains provide evidence for a common geotectonic evolution within the composite Cuyania terrane sharing similar elastic and petrological properties in the Precordilleran and Sierras Pampeanas basement.

Acknowledgements

This research has been supported by the research projects PIP 0072 (G. Vujovich) and PICT 2011-160 from CONICET and the Agencia Nacional de Promoción Científica y Tecnológica from Argentina (ANPCyT). We acknowledege the Incorporated Research Institutions for Seismology (IRIS) for the seismic data used in this study. We thank Doctors Hersh Gilbert and Marianne Marot for their constructive review.

Appendix A. Supplementary data

Supplementary data related to this article can be found at http://dx.doi.org/10.1016/j.jsames.2015.09.005.

References

Alvarado, P., Beck, S., Zandt, G., 2005a. Crustal deformation in the South-Central Andes back-arc terranes as viewed from regional broad-band seismic waveform modelling. Geophys. J. Int. 163 (2), 580–598.

Alvarado, P., Machuca, B.C., Beck, S.L., 2005b. Comparative seismic and petrographic crustal study between the western and eastern Sierras Pampeanas region (31°S). Rev. Asoc. Geol. Argent. 60 (4), 787–796.

Alvarado, P., Beck, S., Zandt, G., 2007. Crustal structure of the South-Central Andes Cordillera and back-arc region from regional waveform modelling. Geophys. J. Int. 170 (2), 858–875.

Alvarado, P., Pardo, M., Gilbert, H., Miranda, S., Anderson, M., Saez, M., Beck, S.L., 2009. Flat-slab subduction and crustal models for the seismically active Sierras

Pampeanas region of Argentina. In: Kay, S., Ramos, V.A., Dickinson, W. (Eds.), MWR204: Backbone of the Americas: Shallow Subduction, Plateau Uplift, and Ridge and Terrane Collision. Geological Society of America, Boulder, Colorado, pp. 261–278.

Alvarado, P., Sánchez, G., Saez, M., Castro de Machuca, B., 2010. Nuevas evidencias de la actividad sísmica del terreno Cuyania en la región de subducción de placa horizontal de Argentina. Rev. Mex. Ciencias Geol. 27 (2), 278–291.

Ammirati, J.B., Alvarado, P., Perarnau, M., Saez, M., Monsalvo, G., 2013. Crustal structure of the Central Precordillera of San Juan, Argentina (31°S) using teleseismic receiver functions. J. S. Am. Earth Sci. 46, 100–109.

Ammirati, J.B., Alvarado, P., Beck, S., 2015. A lithospheric velocity model for the flat slab region of Argentina from joint inversion of Rayleigh wave phase velocity dispersion and teleseismic receiver functions. Geophys. J. Int. 202, 224–241.

Anderson, M., Alvarado, P., Zandt, G., Beck, S.L., 2007. Geometry and brittle deformation of the subducting Nazca Plate, central Chile and Argentina. Geophys. J. Int. 171 (1), 419–434.

Anonymous, 1972. Penrose field conference on Ophiolites. Geotimes 17, 24–25.

Astini, R., 1988. Consideraciones sedimentológicas de la Formación Yerba Loca, Ordovícico de la Precordillera Argentina. 2° Reun. Argent. Sedimentol. 1, 11–15.

Baldis, B., Chebli, G., 1969. Estructura profunda del área central de la Precordillera sanjuanina. 4° Jorn. Geol. Argent. Actas 1, 47–66.

Baldis, B., Beresi, M., Bordonaro, O., Vaca, A., 1982. Síntesis evolutiva de la Precordillera Argentina. 5° Congr. Latinoam. Geol. Actas 4, 399–445.

Banchig, A.L., 1995. Evolución del talud continental Cambro-Ordovícico entre el río San Juan y Los Sombreros, San Juan (Doctoral Thesis). Universidad Nacional de San Juan (inédita), p. 202.

Barazangi, M., Isacks, B.L., 1976. Spatial distribution of earthquakes and subduction of the Nazca plate beneath South America. Geology 4 (11), 686–692. http://dx.doi.org/10.1130/0091-7613(1976).

Basilici, G., Peralta, S., Finney, S.C., 2003. The Portezuelo del Tontal Formation: a widespread storm-dominated siliciclastic shelf of the lower Caradocian, western Precordillera, San Juan Province, Argentina. In: 3rd Latinoamerican Congress of Sedimentology (Abstract), Belem Do Para, Brasil.

Basilici, G., Cutolo, A., Gomes Borges, J.P., Henrique, A., Moretti, P.A., 2005. Ordovician storm-dominated basin and the evolution of the western Gondwana margin (Portezuelo del Tontal, Sierra de La Invernada and Yerba Loca formations, Argentine Precordillera). In: Pankhurst, R.J., Veiga, G.D. (Eds.), Gondwana 12. "Geological and Biological Heritage of Gondwana". Academia Nacional de Ciencias, Mendoza, p. 64. Abstracts.

Beck, S., Zandt, G., Wallace, T., Anderson, M., Fromm, R., Shearer, T., Wagner, L., Koper, K., Alvarado, P., Triep, E., Lince Klinger, F., Araujo, M., Bufaliza, M., Campos, J., Kausel, E., Ruiz, J., 2001. CHARGE, the CHile ARgentinean Geophysical Experiment: Imaging the South Central Andean Lithosphere Using Passive Broadband Seismology. American Geophysical Union. Fall meeting 2001, abstract #T31A-0828.

Bilbao, S.I., 2012. Deformación sísmica de la placa de Nazca en las zonas adyacentes al segmento de subducción horizontal (31°S) utilizando el modelado de ondas sísmicas regionales de banda ancha (Doctoral Thesis). Universidad Nacional de San Juan, Argentina (inédita), p. 114.

Birch, F., 1960. The velocity of compressional waves in rocks to 10 kilobars. J. Geophys. Res. 65, 1083–1102.

Boedo, F.L., Vujovich, G.I., Barredo, S.P., 2012. Caracterización de rocas ultramáficas, máficas y metasedimentarias del cordón del Peñasco, Precordillera occidental, Mendoza. Rev. Asoc. Geol. Argent. 69 (2), 275–285.

Boness, N.L., Zoback, M.D., 2004. Stress-induced seismic velocity and physical properties in the SAFOD Pilot Hole in Parkfield, CA. Geophys. Res. Lett. 31 http://dx.doi.org/10.1029/2003GL019020. L15S17.

Brocher, T.M., 2005. Empirical relations between elastic wave - speeds and density in the Earth's crust. Bull. Seismol. Soc. Am. 95, 2081–2092.

Brocher, T.M., Christensen, N.I., 2001. Density and Velocity Relationships for Digital Sonic and Density Logs from Coastal Washington and Laboratory Measurements of Olympic Peninsula Mafic Rocks and Greywackes. Open-File Rept. 01–264. U.S. Geologycal Survey, p. 39. http://geopubs.wr.usgs.gov/open-file/of01-264/.

Brocher, T.M., Fuis, G.S., Lutter, W.J., Christensen, N.I., Ratchowski, N.A., 2004. Seismic velocity models for the Denali fault zone along the Richardson Highway, Alaska. Bull. Seismol. Soc. Am. 94, S85–S106.

Browning, P., 1984. Cryptic variation within the cumulate sequence of the Oman ophiolite: Magma chamber depth and petrological implications. In: Gass, I.G., Lippard, S.J., Shelton, A.W. (Eds.), Ophiolites and Oceanic Lithosphere, Geological Society of America, Special Publication, vol. 13, pp. 71–82.

Bucher, K., Frey, M., 1994. Petrogenesis of Metamorphic Rocks. Springer-Verlag, Berlin, Heidelberg, New York, p. 318.

Bucher, K., Grapes, R., 2011. Petrogenesis of Metamorphic Rocks. Springer-Verlag, Berlin, Heidelberg, New York, p. 441.

Caballé, M., Furque, G., Cuerda, A., Alfaro, M., 1992. Nuevos hallazgos de graptolitos en la Formación Sierra de La Invernada (Ordovícico), Precordillera de San Juan, Argentina. Ameghiniana 29 (1), 9–26.

Cahill, T., Isacks, B.L., 1992. Seismicity and shape of the subducted Nazca plate. J. Geophys. Res. 97 (B12), 17,503–17,529. http://dx.doi.org/10.1029/92JB00493.

Calkins, J.A., Zandt, G., Gilbert, H., Beck, S.L., 2006. Crustal images from San Juan, Argentina, obtained using high frequency local event receiver functions. Geophys. Res. Lett. 33 (7), L07309.

Castro de Machuca, B., Perarnau, M., Alvarado, P., López, G., Saez, M., 2012. A seismological and petrological crustal model for the southwest of the Sierra de Pie de Palo, Province of San Juan. Rev. Asoc. Geol. Argent. 69, 179–186.

Chernicoff, C., Vujovich, G., Van Staal, C.R., 2009. Geophysical evidence for an extensive Pie de Palo complex mafic-ultramafic belt, San Juan, Argentina. J. S. Am. Earth Sci. 28, 325–332.

Christensen, N.I., 1965. Compressional wave velocities in metamorphic rocks at pressures to 10 kilobars. J. Geophys. Res. 70 (24), 6147–6616.

Christensen, N.I., 1966. Elasticity of ultrabasic rocks. J. Geophys. Res. 71, 5921–5931.

Christensen, N.I., 1978. Ophiolites, seismic velocities and oceanic crustal structure. Tectonophysics 47, 131–157.

Christensen, N.I., 1996. Poisson's ratio and crustal seismology. J. Geophys. Res. 101, 3139–3156.

Christensen, N.I., Fountain, D.M., 1975. Constitution of the lower continental crust based on experimental studies of seismic velocities in granulite. Geol. Soc. Am. Bull. 86, 227–236.

Christensen, N.I., Mooney, W.D., 1995. Seismic velocity structure and composition of the continental crust: a global view. J. Geophys. Res. 100, 9761–9788.

Davis, J., Roeske, S., McClelland, W., Snee, L., 1999. Closing an ocean between the Precordillera terrane and Chilenia: early Devonian ophiolite emplacement and deformation in the southwest Precordillera. In: Ramos, V.A., Keppie, J.D. (Eds.), Laurentia-Gondwana Connections before Pangea, Special Publication, vol. 336. Geological Society of America, pp. 115–138.

DeMets, C., Gordon, R.G., Argus, D.F., 2010. Geologically current plate motions. Geophys. J. Int. 181, 1–80.

Ernst, W.G., 1977. Mineralogic study of eclogitic rocks from Alpe Arami, Lepontine Alps, southern Switzerland. J. Pet. 18, 371–398.

Franzese, J.R., Spalletti, L.A., 2001. Late Triassic–early Jurassic continental extension in southwestern Gondwana: tectonic segmentation and pre-break-up rifting. J. S. Am. Earth Sci. 14 (3), 257–270.

Franzese, J., Spalletti, L., Gómez-Pérez, I., Macdonald, D., 2003. Tectonic and paleoenvironmental evolution of Mesozoic sedimentary basins along the Andean foothills of Argentina (32°–54°S). J. S. Am. Earth Sci. 16 (1), 81–90.

Furque, G., 1983. Descripción Geológica de la Hoja 19c Ciénaga de Gualilán. Boletín Servicio Geológico Argentino, p. 111.

Furque, G., Caballé, M., 1985. Paleozoico inferior en el Cerro Bayo, sierra de la Invernada, San Juan. Revista del Museo de la Plata (Nueva Serie), pp. 1–18 (La Plata, Argentina).

Furque, G., Caballé, M., 1988. Descripción de la sierra de la Invernada, San Juan. Dirección Nacional de Geología y Minería (Inédito), pp. 1–76 (Buenos Aires, Argentina).

Furque, G., Cuerda, A.J., Alfaro, M., 1990. El Ordovícico de la Sierra de la Invernada y su fauna de graptolitos, San Juan. Revista del Museo de la Plata (Nueva Serie). In: Paleontología, IX, pp. 159–181 (La Plata, Argentina).

Gans, C.R., Beck, S.L., Zandt, G., Gilbert, H., Alvarado, P., Anderson, M., Linkimer, L., 2011. Continental and oceanic crustal structure of the Pampean flat slab region, western Argentina, using receiver function analysis: new high-resolution results. Geophys. J. Int. 186, 45–58.

Gilbert, H., Beck, S., Zandt, G., 2006. Lithosperic and upper mantle structure of Central Chile and Argentina. Geophys. J. Int. 165, 383–398.

Gomes, J.P.B., Basilici, G., Cutolo, A.A., Henrique, A., Moretti Jr., P.A., 2005. The importance of storm-gravitational combined flows on the construction of sandstone reservoirs in siliciclastic shelves: analogous in Portezuelo del Tontal and Sierra de la Invernada Formations (middle-upper Ordovician, Precordillera Argentina). Gondwana 12 "Geological and Biological Heritage of Gondwana", Mendoza, Argentina. Academia Nacional de Ciencias, p. 174. Abstracts.

Hacker, B.R., 1996. Eclogite Formation and the Rheology, Buoyancy, Seismicity, and H2O Content of Oceanic Crust. In: Geophysical Monograph, vol. 96. American Geophysical Union, pp. 171–178. http://dx.doi.org/10.1029/GM096p0337. Washington, D. C. USA.

Hacker, B.R., Abers, G.A., Peacock, S.M., 2003. Subduction factory 1. Theoretical mineralogy, density, seismic wave speeds, and H_2O content. J. Geophys. Res. 108 (B1), 2029. http://dx.doi.org/10.1029/2001JB001127.

Hacker, B., Abers, G., 2004. Subduction factory 3: an excel worksheet and macro for calculating the densities, seismic wave speeds, and H_2O contents of minerals and rocks at pressure and temperature. Geochem. Geophys. Geosyst. G3. Tech. Brief. 5 (1) http://dx.doi.org/10.1029/2003GC000614.

Haller, M.J., Ramos, V.A., 1984. Las ofiolitas famitinianas (Eopaleozoico) de las provincias de San Juan y Mendoza. 9° Congr. Geol. Argent. Actas 3, 66–83 (San Carlos de Bariloche, Argentina).

Herrmann, R.B., Ammon, C.J., 2002. Computer Programs in Seismology: Surface Waves, Receiver Functions and Crustal Structure. www.eas.slu.edu/People/RBHerrmann/CPS330.html.

Holbrook, W.S., Gajewski, D., Krammer, A., Prodehl, C., 1988. An interpretation of wide-angle compressional and shear wave data in Southwest Germany: Poisson's ratio and petrological implications. J. Geophys. Res. 93, 12081–12106. http://dx.doi.org/10.1029/88JB03099.

Holbrook, W.S., Mooney, W.D., Christensen, N.I., 1992. The seismic velocity structure of the deep continental crust. In: Fountain, D.M., Arculus, R., Kay, R. (Eds.), Lower Continental Crust. Elsevier, New York, USA, pp. 1–43.

Jackson, J., Austrheim, H., McKenzie, D., Priestley, K., 2004. Metastability, mechanical strength, and the support of mountain belts. Geology 32, 625–628.

Johnson, J.E., Christensen, N.I., 1992. Shear wave reflectivity, anisotropies, Poisson's ratios, and densities of a southern Appalachian Paleozoic sedimentary sequence. Tectonophysics 210, 1–20.

Julià, J., Ammon, C.J., Herrmann, R.B., Correig, A.M., 2000. Joint inversion of receiver function and surface wave dispersion observations. Geophys. J. Int. 143, 99–112.

Please cite this article in press as: Pérez Luján, S.B., et al., Constraining a mafic thick crust model in the Andean Precordillera of the Pampean flat slab subduction region, Journal of South American Earth Sciences (2015), http://dx.doi.org/10.1016/j.jsames.2015.09.005

Kay, S.M., Maksaev, V., Mpodozis, C., Moscoso, R., Nasi, C., 1988. Tertiary Andean magmatism in Argentina and Chile between 28°-33°S: correlation of magmatic chemistry with a changing Benioff zone. J. S. Am. Earth Sci. 1, 21–38.

Kay, S.M., Orrell, S., Abruzzi, J.M., 1996. Zircon and whole rock Nd–Pb isotopic evidence for a Grenville age and Laurentia origin for the basament of the Precordilleran terrane in Argentina. J. Geol. 104, 637–648.

Kroenke, L.W., Manghnani, M.H., Rai, C.S., Fryer, P., Ramananantoandro, R., 1976. Elastic properties of selected ophiolite rocks from Papua New Guinea: nature and composition of oceanic lower crust and upper mantle. In: Sutton, G.H., Manghnani, M.H., Moberly, R. (Eds.), The Geophysics of the Pacific Ocean Basin and its Margins, A.G.U. Monograph, vol. 19, pp. 407–422 (Washington, D.C).

Langston, C.A., 1979. Structure under Mount Rainier, Washington, inferred from teleseismic body waves. J. Geophys. Res. 84, 4749–4762.

Leveratto, M.A., 1968. Geología del oeste de Ullum-Zonda, borde oriental de la Precordillera de San Juan. Rev. Asoc. Geol. Argent. 23 (2), 129–157.

Le Maitre, R.W., 1989. A Classification of Igneous Rocks and Glossary of Terms. Blackwell, Oxford, United Kingdom, pp. 1–193.

Lippard, S.J., Shelton, A.W., Gass, I.G., 1986. The Ophiolite of Northern Oman, Geological Society of London, Memoirs, 11. Blackwell Scientific, Oxford, United Kingdom, p. 178.

Mackwell, S.J., Zimmerman, M.E., Kohlstedt, D.L., 1998. High temperature deformation of dry diabase with application to tectonics on Venus. J. Geophys. Res. 103, 975–984.

Mavko, G., Mukerji, T., Dvorkin, J., 1998. The Rock Physics Handbook: Tools for Seismic Analysis in Porous Media. Cambridge University Press, Cambridge, England, p. 329.

Marot, M., Monfret, T., Gerbault, M., Nolet, G., Ranalli, G., Pardo, M., 2014. Flat versus normal subduction zones: a comparison based on 3-D regional traveltime tomography and petrological modelling of central Chile and western Argentina (29°–35°S). Geophys. J. Int. 199, 1633–1654.

McDonough, M.R., Ramos, V.A., Isachsen, C.E., Bowring, S.A., Vujovich, G.I., 1993. Edades preliminares de circones del basamento de la Sierra de Pie de Palo, Sierras Pampeanas Occidentales de San Juan: Sus implicancias para el supercontinente Proterozoico de Rodinia. In: Proceedings of the 12th Congreso Geológico Argentino and 2nd Congreso de Exploración de Hidrocarburos, Mendoza, Argentina, vol. 3, pp. 340–342.

Monsalvo, G., Alvarado, P., Saez, M., Linkimer, L., Bilbao, I., 2014. Deformación sísmica reciente de la sierra de Pie de palo, provincia de San Juan. Rev. Asoc. Geol. Argent. 71 (2), 260–266.

Moretti, P.A., 2009. Análise de fácies e modelo paleodeposicional da plataforma siliciclástica ordoviciana da Pré-Cordilheira Argentina. In: Subcomissão de Pós-graduação em Ciências e Engenharia de petróleo. Faculdade de Engenharia Mecânica e Instituto de Geociências, Universidade Estadual de Campinas, São Paulo, Brasil, p. 126.

Ortega, G., Albanesi, G.L., Banchig, A.L., Peralta, G.L., 2008. High resolution conodont-graptolite biostratigraphy in the Middle-Upper Ordovician of the Sierra de la Invernada Formation (Central Precordillera, Argentina). Geol. Acta 2, 161–180.

Ortiz, A., Zambrano, J.J., 1981. La provincia geológica Precordillera oriental. 8° Congr. Geol. Argent. Actas 3, 59–74 (San Luis, Argentina).

Pardo, M., Comte, D., Monfret, T., 2002. Seismotectonic and stress distribution in the central Chile subduction zone. J. S. Am. Earth Sci. 15 (1), 11–22.

Perarnau, M., Alvarado, P., Saez, M., 2010. Estimación de la estructura cortical de velocidades sísmicas en el suroeste de la Sierra de Pie de Palo, Provincia de San Juan. Rev. Asoc. Geol. Argent. 67 (4), 473–480.

Perarnau, M., Gilbert, H., Alvarado, P., Martino, R., Anderson, M., 2012. Crustal structure of the Eastern Sierras Pampeanas of Argentina using high frequency local receiver functions. Tectonophysics 580, 208–217.

Pérez Luján, S., Ammirati, J.B., Alvarado, P., Vujovich, G., 2013. New petrological and seismological crustal model of the Sierra de la Invernada, Central Precordillera of San Juan (31°S), Argentina. Boll. Geofis. 54 (2), 92–95.

Peterson, J.J., Fox, P.J., Schreiber, E., 1974. Newfoundland ophiolites and the geology of the oceanic layer. Nature 247, 194–196.

Poster, C.K., 1973. Ultrasonic velocities in rocks from the Troodos massif, Cyprus. Nature 243, 2–3.

Ramos, V.A., 1988. Tectonics of the late Proterozoic–early Paleozoic: a collisional history of southern South America. Episodes 11 (3), 168–174.

Ramos, V.A., 1994. Terranes of southern Gondwanaland and their control in the Andean structure (30°–33°S latitude). In: Reutter, K.J., Scheuber, E., Wigger, P.J. (Eds.), Tectonics of the Southern Central Andes. Springer-Verlag, New York, USA, pp. 249–261.

Ramos, V.A., Jordan, T.E., Allmendinger, R.W., Mpodozis, C., Kay, S.M., 1984. Chilenia: un terreno alóctono en la evolución de los Andes centrales. 9° Congr. Geol. Argent. Actas 2, 84–106 (San Carlos de Bariloche, Argentina).

Ramos, V.A., Jordan, T.E., Allmendinger, R.W., Mpodozis, C., Kay, S.M., Cortés, M., Palma, M., 1986. Paleozoic terranes of the central Argentine-Chilean Andes. Tectonics 5, 855–880.

Ramos, V.A., Cristallini, E.O., Pérez, D.J., 2002. The Pampean flat slab of the central Andes. J. S. Am. Earth Sci. 15, 59–78. http://dx.doi.org/10.1016/S08959811 (02) 000068.

Rapela, C.W., Pankhurst, R.J., Casquet, C., Baldo, E., Galindo, C., Fanning, C.M., Dahlquist, J.M., 2010. The Western Sierras Pampeanas: protracted Grenville-age history (1330—1030 Ma) of intra-oceanic arcs, subduction-accretion at continental-edge and AMCG intraplate magmatism. J. S. Am. Earth Sci. 29, 105–127.

Regnier, M., Chatelain, J.L., Smalley Jr., R., Chiu, J.M., Isacks, B., Araujo, M., 1992. Seismotectonics of Sierra Pie de Palo, a basement block upflit in the Andean foreland of Argentina. Bull. Seismol. Soc. Am. 82 (6), 2549–2571.

Robinson, D., Bevins, R.E., Rubinstein, N., 2005. Subgreenschist facies metamorphism of metabasites from the Precordillera terrane of western Argentina; constraints on the later stages of accretion onto Gondwana. Eur. J. Mineral. 17, 441–452.

Rubinstein, N., Bevins, R., Robinson, D., Morello, O., 1998. Very low metamorphism in the Alcaparrosa Formation, western Precordillera, Argentina. 10° Congr. Latinoam. Geol. 6° Congr. Nac. Geol. Econ., Actas 2, 326–329 (Buenos Aires, Argentina).

Rybacki, E., Gottschalk, M., Wirth, R., Dresen, G., 2006. Influence of water fugacity and activation volume on the flow properties of fine-grained anorthite aggregates. J. Geophys. Res. 111, B03203. http://dx.doi.org/10.1029/2005JB003663.

SIEMBRA, 2015. www.geo.arizona.edu/SIEMBRA.

Smalley Jr., R., Pujol, J., Regnier, M., Chiu, J.M., Chatelain, J.L., Isacks, B.L., Araujo, M., Puebla, N., 1993. Basement seismicity beneath the Andean Precordillera thin-skinned thrust belt and implications for crustal and lithospheric behaviour. Tectonics 12, 63–76.

Spalletti, L.A., Cingolani, C.A., Varela, R., Cuerda, A.J., 1989. Sediment gravity flow deposits of an Ordovician deep-sea fan system (western Precordillera, Argentina). Sediment. Geol. 61, 287–301.

Tassara, A., Götze, H.J., Schmidt, S., Hackney, R., 2006. Three-dimensional density model of the Nazca plate and the Andean continental margin. J. Geophys. Res. 111 http://dx.doi.org/10.1029/2005JB003976.

Vujovich, G., Kay, S.M., 1998. A Laurentian? Grenville age oceanic arc/backarc terrane in the Sierra de Pie de Palo, western Sierras Pampeanas, Argentina. In: Pankhurst, R.J., Rapela, C.W. (Eds.), The Proto Andean Margin of Gondwana, Geological Society of London Special Publication, vol. 142, pp. 159–180.

Vujovich, G.I., Van Staal, C.R., Davis, W., 2004. Age constraints on the tectonic evolution and provenance of the Pie de Palo Complex, Cuyania composite terrane, and the Famatinian orogeny in the Sierra de Pie de Palo, San Juan, Argentina. In: Vujovich, G.I., Fernandes, L.A.D., Ramos, V.A. (Eds.), Cuyania, an Exotic Block to Gondwana. Gondwana Research, vol. 7(4), pp. 1041–1056.

Wagner, L.S., Beck, S.L., Zandt, G., 2005. Upper mantle structure in the south central Chilean subduction zone (30° to 36°S). J. Geophys. Res. 110 http://dx.doi.org/10.1029/2004JB003238.

Wang, Y.F., Zhang, J.F., Jin, Z.M., Green II, H.W., 2012. Mafic granulite rheology: implications for a weak continental lower crust. Earth Planet. Sci. Lett. 353, 99–107.

Watson, D.F., 1982. Acord: automatic contouring of raw data. Comput. Geosci. 8, 97–101.

White, R.S., McKenzie, D., O'Nions, R.K., 1992. Oceanic crustal thickness from seismic measurements and rare earth element inversions. J. Geophys. Res. 97, 19,683–19,715.

Willner, A.P., Gerdes, A., Massonne, H.J., Schmidt, A., Sudo, M., Thomson, S.N., Vujovich, G., 2011. The geodynamics of collision of a microplate (Chilenia) in Devonian times deduced by the pressure-temperature-time evolution within part of a collisional belt (Guarguaraz Complex, W-Argentina). Contribu. Mineral. Pet. 162, 303–327.

Whitney, D., Evans, B., 2010. Abbreviations for names of rock-forming minerals. Am. Mineral. 95, 185–187.

Yang, X., Deloule, E., Xia, Q., Fan, Q., Feng, M., 2008. Water contrast between Precambrian and Phanerozoic continental lower crust in eastern China. J. Geophys. Res. 113, B08207.

Yardley, B.W.D., 1989. An Introduction to Metamorphic Petrology. London. Longman, Earth Sciences Series, New York. USA, p. 248.

Yardley, B.W.D., Valley, J.W., 1997. The petrologic case for a dry lower crust. J. Geophys. Res. 102, 12173–12185.

Yañez, G.A., Ranero, C.R., Von Huene, R., Diaz, J., 2001. Magnetic anomaly interpretation across the southern Central Andes (32 degrees–34 degrees S); the role of the Juan Fernandez Ridge in the late tertiary evolution of the margin. J. Geophys. Res. 106 (B4), 6325–6345.

Zhang, J., Green, H.W., 2007. Experimental investigation of eclogite rheology and its fabrics at high temperature and pressure. J. Metamorph. Geol. 25, 97–115.

Please cite this article in press as: Pérez Luján, S.B., et al., Constraining a mafic thick crust model in the Andean Precordillera of the Pampean flat slab subduction region, Journal of South American Earth Sciences (2015), http://dx.doi.org/10.1016/j.jsames.2015.09.005